The molecular mechanisms by which the MMP activation regulates METH-induced increase in extracelluar dopamine levels remain to be elucidated. It has been demonstrated that reverse activation and internalization of plasmalemmal DAT is involved in the METH-induced increase in extracellular dopamine levels (Sulzer *et al.* 1995; Khoshbouei *et al.* 2004). The degradation of ECM and other substrates by MMP may result in conformational and/or functional changes in plasma membrane proteins (Bixby *et al.* 1994; Sunderland *et al.* 2000; Kaczmarek *et al.* 2002). Recently, it was reported that association of membrane type 5-MMP with AMPA receptor binding protein can influence axon pathfinding or synapse remodelling through proteolysis of cadherins in neuron (Monea *et al.* 2006). Consistently, we demonstrated that [^{3}H]dopamine uptake into striatal synaptosomes was reduced in wild-type mice after repeated METH treatment, but METH-induced changes in [^{3}H]dopamine uptake were significantly attenuated in MMP-2-(−/−) and MMP-9-(−/−) mice (Fig. 6). These results suggest that the MMP-2 and MMP-9 may regulate the METH-induced increase in the extracellular dopamine levels by modulating DAT activity through the degradation of ECM. Alternatively, MMPs are reported to activate neurotrophic factors such as insulin-like growth factor-1 (Fowlkes *et al.* 1995) and fibroblast growth factor (Levi *et al.* 1996). Thus, it is possible that MMP-2 and MMP-9 may play a role in development of METH dependence by modulating the activity of these neurotrophic factors.

In conclusion, we have demonstrated for the first time that repeated but not acute METH treatment induces increased MMP-2 and MMP-9 expression in neurons and/or glial cells in the Fc and NAc. The net increase in MMP activity may be responsible at least in part for the development of METH-induced behavioural plasticity. Additionally, it is noticed that while the effects shown in the Fc and NAc are likely to represent METH-induced changes in MMP activity that are specific to reward areas, these changes might also be found in other brain regions, such as hippocampus and striatum, that are not specifically associated with METH reward, indicating the possibility that MMP changes are not specificity of the response to METH reward circuit. Further work would be required to completely resolve this important issue. Consistently, deletion of the MMP-2 or MMP-9 gene resulted in the attenuation of METH-induced behavioural sensitization and CPP in mice. We also provided pharmacological and genetic evidence that MMP-2 and MMP-9 are involved in the regulation of METH-induced changes in dopamine release and uptake in the NAc. These results, together with the well-known function of the MMPs to degrade ECM, suggest that repeated METH-induced overexpression of MMP-2 and MMP-9 plays a crucial role in functional and possibly structural changes in the Fc and NAc, which are related to METH-induced behavioural sensitization and reward.

Acknowledgements

This study was supported in part by Grants-in-Aid for Scientific Research (no. 18790052), the 21st Century COE Program from the Ministry of Education, Culture, Sports, Science and Technology of Japan, Health Sciences Research from the Ministry of Health, Labour and Welfare of Japan, Special Coordination Funds for Promoting Science and Technology, Target-Oriented Brain Science Research Program from the Ministry of Education, Culture, Sports, Science and Technology of Japan, and an SRF Grant for Biomedical Research.

References

Asahi M., Wang X., Mori T., Sumii T., Jung J. C., Moskowitz M. A., Fini M. E. and Lo E. H. (2001) Effects of matrix metalloproteinases-9 gene knock-out on the proteolysis of blood–brain barrier and white matter components after cerebral ischemia. *J. Neurosci.* **21**, 7724–7732.

Baricos W. H., Cortez S. L., el-Dahr S. S. and Schnaper H. W. (1995) ECM degradation by cultured human mesangial cells is mediated by a PA/plasmin/MMP-2 cascade. *Kidney Int.* **47**, 1039–1047.

Berke J. and Hyman S. T. (2000) Addiction, dopamine, and the molecular mechanisms of memory. *Neuron* **25**, 515–532.

Bixby J., Grunwald G. B. and Bookman R. J. (1994) Ca^{2+} influx and neurite growth in response to purified N-cadherin and laminin. *J. Cell Biol.* **127**, 1461–1475.

Cervinski M. A., Foster J. D. and Vaughan R. A. (2005) Psychoactive substrates stimulate dopamine transporter phosphorylation and down-regulation by cocaine-sensitive and protein kinase C-dependent mechanisms. *J. Biol. Chem.* **280**, 40 442–40 449.

Fowlkes J. L., Thrailill K. M., Serra D. M., Suzuki K. and Nagase H. (1995) Matrix metalloproteinases as insulin-like growth factor binding protein-degrading proteinases. *Prog. Growth Factor Res.* **6**, 255–263.

Franklin K. B. J. and Paxinos G. (1997) *The Mouse Brain in Stereotaxic Coordinates*. San Diego: Academic Press.

Itoh T., Ikeda T., Gomi H., Nakao S., Suzuki T. and Itohara S. (1997) Unaltered secretion of β-amyloid precursor protein in gelatinase A (matrix metalloproteinases 2)-deficient mice. *J. Biol. Chem.* **272**, 22 389–22 392.

Kaczmarek L., Lapinska-Dzwonek J. and Szymczak S. (2002) Matrix metalloproteinases in the adult brain physiology: a link between c-Fos, AP-1 and remodeling of neuronal connections? *EMBO J.* **21**, 6643–6648.

Khoshbouei H., Sen N., Guptaroy B., Johnson L., Lund D., Gnegy M. E., Galli A. and Javitch J. A. (2004) N-terminal phosphorylation of the dopamine transporter is required for amphetamine-induced efflux. *PLoS Biol.* **2**, 387–393.

Krekoski C. A., Neubauer D., Graham J. B. and Muir D. I. (2002) Metalloproteinase-dependent predegeneration *in vitro* enhances axonal regeneration within a cellular peripheral nerve grafts. *J. Neurosci.* **22**, 10 408–10 415.

Lee S. R., Tsuji K., Lee S. R. and Lo E. H. (2004) Role of matrix metalloproteinases in delayed neuronal damage after transient global cerebral ischemia. *J. Neurosci.* **24**, 671–678.

Levi E., Fridman R., Miao H.-Q., Ma Y. S., Yayon A. and Vlodavsky I. (1996) Matrix metalloproteinases-2 releases active soluble ectodomain of fibroblast growth factor receptor 1. *Proc. Natl Acad. Sci. USA* **93**, 7069–7074.

Lo E. H., Wang X. and Cuzner M. L. (2002) Extracellular proteolysis in brain injury and inflammation: role for plasminogen activators and matrix metalloproteinases. *J. Neurosci. Res.* **69**, 1–9.

Mizoguchi H., Yamada K., Mizuno M., Mizuno T., Nitta A., Noda Y. and Nabeshima T. (2004) Regulations of methamphetamine reward by extracellular signal-regulated kinase 1/2/ets-like gene-1 signaling pathway via the activation of dopamine receptors. *Mol. Pharmacol.* **65**, 1293–1301.

Monard D. (1988) Cell-derived proteases and protease inhibitors as regulators of neurite outgrowth. *Trends Neurosci.* **11**, 541–544.

Monea S., Jordan B. A., Srivastava S., DeSouza S. and Ziff E. B. (2006) Membrane localization of membrane type 5 matrix metalloproteinases by AMPA receptor binding protein and cleavage of cadherins. *J. Neurosci.* **22**, 2300–2312.

Nagai T., Yamada K., Yoshimura M., Ishikawa K., Miyamoto Y., Hashimoto K., Noda Y., Nitta A. and Nabeshima T. (2004) The tissue plasminnogen activator-plasmin system participates in the rewarding effect of morphine by regulating dopamine release. *Proc. Natl Acad. Sci. USA* **101**, 3650–3655.

Nagai T., Noda Y., Ishikawa K., Miyamoto Y., Yoshimura M., Ito M., Takayanagi M., Takuma K., Yamada K. and Nabeshima T. (2005) The role of tissue plasminogen activator in methamphetamine-related reward and sensitization. *J. Neurochem.* **92**, 660–667.

Nagase H. and Woessner J. F. Jr (1999) Matrix metalloproteinases. *J. Biol. Chem.* **274**, 21 491–21 494.

Nagy V., Bozdagi O., Matynia A., Balcerzyk M., Okulski P., Dzwonek J., Costa R. M., Silva A. J., Kaczmarek L. and Huntley G. W. (2006) Matrix metalloproteinase-9 is required for hippocampal late-phase long-term potentiation and memory. *J. Neurosci.* **15**, 1923–1934.

Nakajima A., Yamada K., Nagai T. *et al.* (2004) Role of tumor necrosis factor-α in methamphetamine-induced drug dependence and neurotoxicity. *J. Neurosci.* **24**, 2212–2225.

Nestler E. J. (2001) Molecular basis of long-term plasticity underlying addiction. *Nat. Rev. Neurosci.* **2**, 119–128.

Paxinos G. and Watson C. (1982) *The Rat Brain in Stereotaxic Coordinates*. New York: Academic Press.

Reeves T., Prins M. L., Zhu J. P., Povlishock J. T. and Phillips L. L. (2003) Matrix metalloproteinases inhibition alters functional and structural correlates of deafferentation-induced sprouting in the dentate gyrus. *J. Neurosci.* **12**, 10 182–10 189.

Robinson T. E. and Kolb B. (1997) Persistent structural modifications in nucleus accumbens and prefrontal cortex neurons produced by previous experience with amphetamine. *J. Neurosci.* **17**, 8491–8497.

Shippenberg T. S. and Heidbreder Ch (1995) Sensitization to the conditioned rewarding effects of cocaine: pharmacological and temporal characteristics. *J. Pharmacol. Exp. Ther.* **273**, 808–815.

Sulzer D., Chen T. K., Lau Y. Y., Kristensen H., Rayport S. and Ewing A. (1995) Amphetamine redistributes dopamine from synaptic vesicles to the cytosol and promotes reverse transport. *J. Neurosci.* **15**, 4102–4108.

Sunderland W. J., Son Y. J., Miner J. H., Sanes J. R. and Carlson S. S. (2000) The presynaptic calcium channel is part of a transmembrane complex linking a synaptic laminin ($\alpha 4\beta 2\gamma 1$) with non-erythroid spectrin. *J. Neurosci.* **20**, 1009–1019.

Szklarczyk A., Lapinska J., Rylski M., Mckay R. D. and Kaczmarek L. (2002) Matrixmetalloproteinase-9 undergoes expression and activation during dendritic remodeling in adult hippocampus. *J. Neurosci.* **22**, 920–930.

Uhm J. H., Dolley N. P., Oh L. Y. and Yong V. W. (1998) Oligodendrocytes utilize a matrix metalloproteinases, MMP-9, to extend processes along an astrocyte extracellular matrix. *Glia* **22**, 53–63.

Vaillant C., Didier-Bazes M., Hurter A., Bein M. F. and Thomasset N. (1999) Spatiotemporal expression patterns of metalloproteinases and their inhibitors in the post-natal developing rat cerebellum. *J. Neurosci.* **19**, 4994–5004.

Wang X., Lee S. R., Arai K., Lee S. R., Tsuji K., Rebeck G. W. and Lo E. H. (2003) Lipoprotein receptor-mediated induction of matrix metalloproteinase by tissue plasminogen activator. *Nat. Med.* **9**, 1313–1317.

Wright J. W., Reichert J. R., Davis C. J. and Harding J. W. (2002) Neural plasticity and the brain renin-angiotensin system. *Neurosci. Biobehav. Rev.* **26**, 529–552.

Yamada K., Nagai T. and Nabeshima T. (2005) Drug dependence, synaptic plasticity, and tissue plasminogen activator. *J. Pharmacol. Sci.* **97**, 157–161.

Yong V. W., Power C., Forsyth P. and Edwards D. R. (2001) Metalloproteinases in biology and pathology of the nervous system. *Nat. Rev. Neurosci.* **2**, 502–511.

Zahniser N. R. and Sorkin A. (2004) Rapid regulation of the dopamine transporter: role in stimulant addiction? *Neuropharmacology* **47**, 80–91.

Zhang J. W. and Gottschall P. E. (1997) Zymographic measurement of gelatinase activiy in brain tissue after detergent extraction and affinity-support purification. *J. Neurosci. Meth.* **76**, 15–20.

Journal of Neurochemistry, 2007, **102**, 1548–1560 doi:10.1111/j.1471-4159.2007.04623.x

Role of matrix metalloproteinase and tissue inhibitor of MMP in methamphetamine-induced behavioral sensitization and reward: implications for dopamine receptor down-regulation and dopamine release

Hiroyuki Mizoguchi,*,† Kiyofumi Yamada,*,† Akihiro Mouri,* Minae Niwa,* Tomoko Mizuno,* Yukihiro Noda,*,§ Atsumi Nitta,* Shigeyoshi Itohara,¶ Yoshiko Banno‡ and Toshitaka Nabeshima*,**

**Department of Neuropsychopharmacology and Hospital Pharmacy, Nagoya University Graduate School of Medicine, Nagoya, Japan*

†Laboratory of Neuropsychopharmacology, Division of Life Sciences, Graduate School of Natural Science & Technology, Kanazawa University, Kanazawa, Japan

‡Department of Cell Signaling, Gifu University Graduate School of Medicine, Gifu, Japan

§Division of Clinical Science in Clinical Pharmacy Practice, Management and Research, Faculty of Pharmacy, Meijo University, Nagoya, Japan

¶Laboratory for Behavioral Genetics, RIKEN Brain Science Institute, Wako, Japan

***Department of Chemical Pharmacology, Graduate School of Pharmaceutical Sciences, Meijo University, Nagoya, Japan*

Abstract

Matrix metalloproteinases (MMPs) and its inhibitors (TIMPs) function to remodel the pericellular environment. We have demonstrated that methamphetamine (METH)-induced behavioral sensitization and reward were markedly attenuated in MMP-2- and MMP-9 deficient [MMP-2-(−/−) and MMP-9-(−/−)] mice compared with those in wild-type mice, suggesting that METH-induced expression of MMP-2 and MMP-9 in the brain plays a role in the development of METH-induced sensitization and reward. In the present study, we investigated the changes in TIMP-2 expression in the brain after repeated METH treatment. Furthermore, we studied a role of MMP/TIMP system in METH-induced behavioral changes and dopamine neurotransmission. Repeated METH treatment induced behavioral sensitization, which was accompanied by an increase in TIMP-2 expression. Antisense TIMP-2 oligonucleotide (TIMP-AS) treatment enhanced the sensitization, which was associated with the potentiation of METH-induced dopamine release in the nucleus accumbens (NAc). On the other hand, MMP-2/-9 inhibitors blocked the METH-induced behavioral sensitization and conditioned place preference, a measure of the rewarding effect, and reduced the METH-increased dopamine release in the NAc. Dopamine receptor agonist-stimulated [^{35}S]GTPγS binding was reduced in the frontal cortex of sensitized rats. TIMP-AS treatment potentiated, while MMP-2/-9 inhibitor attenuated, the reduction of dopamine D2 receptor agonist-stimulated [^{35}S]GTPγS binding. Repeated METH treatment also reduced dopamine D2 receptor agonist-stimulated [^{35}S]GTPγS binding in wild-type mice, but such changes were significantly attenuated in MMP-2-(−/−) and MMP-9-(−/−) mice. These results suggest that the MMP/TIMP system is involved in METH-induced behavioral sensitization and reward, by regulating dopamine release and receptor signaling.

Keywords: dopamine, dopamine receptor, matrix metalloproteinase, methamphetamine, tissue inhibitor of matrix metalloproteinase.

J. Neurochem. (2007) **102**, 1548–1560.

Received December 26, 2006; revised manuscript received March 9, 2007; accepted March 12, 2007.

Address correspondence and reprint requests to Toshitaka Nabeshima, Ph.D., Department of Neuropsychopharmacology and Hospital Pharmacy, Nagoya University Graduate School of Medicine, Showa-ku, Nagoya 466-8560, Japan, or Department of Chemical Pharmacology, Graduate School of Pharmaceutical Sciences, Meijo University, Tempaku-ku, Nagoya 468-8503, Japan. E-mail: tnabeshi@med.nagoya-u.ac.jp, or Kiyofumi Yamada, Ph.D., Laboratory of Neuropsychopharmacology, Division of Life Sciences, Graduate School of Natural Scinece, and Technology, Kanazawa University, Kakuma-machi, Kanazawa 920-1192, Japan. E-mail: kyamada@p.kanazawa-u.ac.jp

Abbreviations used: CPP, conditioned place preference; ECM, extracellular matrix; Fc, frontal cortex; GDP, guanosine-5′-diphosphate; METH, methamphetamine; MMP, matrix metalloproteinases; NAc, nucleus accumbens; TIMPs, tissue inhibitors of metalloproteinase.

Drug dependence is a complex phenomenon with important psychological and social causes and consequences, which may be associated with neural plasticity and remodeling of specific brain circuits caused by repeated exposure to drugs of abuse (Shippenberg and Heidbreder 1995; Berke and Hyman 2000; Yamada *et al.* 2005). Methamphetamine (METH), a common drug of abuse, has both acute and long-lasting effects on psychomotor behaviors. Although the involvement of various endogenous substances such as TNF-α (Nakajima *et al.* 2004), tissue plasminogen activator (tPA) (Nagai *et al.* 2004, 2005) and brain-derived neurotrophic factor (Nestler 2001), which are known to play a role in synaptic plasticity, has been implicated in the development of METH-induced behavioral sensitization and reward (Shippenberg and Heidbreder 1995; Robinson and Kolb 1997; Mizoguchi *et al.* 2004), the mechanism underlying psychostimulant-induced remodeling of synaptic structures remains to be determined.

Tissue inhibitors of metalloproteinase (TIMPs) belong to a family of multifunctional secreted proteins (TIMP-1–4) that regulate the proteolytic activity of matrix metalloproteinases (MMPs), and possess growth-promoting and cell cycle-regulating activities in various cell types (Mannello and Gazzanelli 2001). MMP and TIMP function to modulate functional and structural remodeling of cellular architecture in the context of pathophysiology primarily through the cleavage of extracellular matrix (ECM) proteins, bioavailability of growth factors and cytokines, and shedding of membrane receptors (Sternlicht and Werb 2001; Yong *et al.* 2001). It has been recently demonstrated that neuronal TIMP-1 (Rivera *et al.* 1997) and MMP-9 (Szklarczyk *et al.* 2002) are regulated by synaptic activity, suggesting that the balance between MMPs and TIMPs is important in the activity-dependent re-organization of the neuronal architecture with possible effects on synaptic physiology. Thus, the MMP/TIMP ratio and net MMP activity may be involved in brain development, because extensive cellular migration and remodeling of the ECM are necessary for neural development (Vaillant *et al.* 1999; Wright *et al.* 2002).

We have recently demonstrated that repeated but not acute METH treatment increases the expression of both MMP-2 and MMP-9 in neurons and/or glial cells in the frontal cortex (Fc) and nucleus accumbens (NAc), and that deletion of the MMP-2 [MMP-2-(−/−) mice] or MMP-9 gene [MMP-9-(−/−) mice] resulted in the attenuation of METH-induced sensitization and reward in mice. We also provided genetic evidence that the MMP expression is involved in the regulation of METH-induced changes in dopamine release and uptake in the NAc. Based on these findings, we have proposed that MMP-2 and MMP-9 are involved in METH-induced synaptic plasticity and related behavioral changes (Mizoguchi *et al.* 2007).

In the present study, we further investigated whether the MMP/TIMP system is involved in METH-induced behavioral sensitization and reward in rat. In this study, we show that TIMP-2 expression is induced by repeated METH treatment in the brain, and that the MMP/TIMP system is involved in the development of METH-induced behavioral sensitization and reward. Inhibition of TIMP-2 function enhanced whereas MMP inhibitors reduced the METH-induced dopamine release and the down-regulation of dopamine receptor agonist-stimulated [^{35}S]GTPγS binding.

Materials and methods

Animals

Male Wistar rats (8-weeks old; Charles River Japan, Yokohama, Japan) weighing 270 ± 20 g at the beginning of experiments were used in the study. We also used MMP-2 homozygous knock-out [MMP-2-(−/−)] and their wild-type (C57BL/6 J) mice (10–12 weeks old). The mutant mice were backcrossed into the C57BL/6 J strain more than thirteen times, and the generation, genotyping, and characterization of MMP-2-(−/−) mice have been described (Itoh *et al.* 1997). MMP-9 homozygous knock-out [MMP-9-(−/−)] mice (10–12-weeks old) were obtained from the Jackson Laboratory (Bar Harbor, ME, USA), and crossed to FVB/N mice for five generations before being made homozygous. Wild-type FVB/N [MMP-9-(+/+)] mice were obtained from the CLEA Japan (Fuji, Japan).

All experiments were performed in accordance with the Guidelines for Animal Experiments of the Nagoya University School of Medicine, the Guiding Principles for the Care and Use of Laboratory Animals approved by the Japanese Pharmacological Society, and the United States National Institutes of Health Guide for the Care and Use of Laboratory Animals.

METH treatment for behavioral sensitization

Rats were given saline or METH at a dose of 2 mg/kg (s.c.) for 5 days (n = 7–8) (Nakajima *et al.* 2004; Nagai *et al.* 2005; Mizoguchi *et al.* 2007). Rats were placed in their home cage for 1 h following injection and then locomotor activity was measured in an acrylic chamber (25 × 42 × 20 cm) for 1 h using behavioral analysis systems (SCANET SV-10: Neuroscience, Tokyo, Japan) on day 1, 3 and 5.

Conditioned place preference

The apparatus used for the place conditioning task consisted of two compartments: a black Plexiglas box and a transparent Plexiglas box (both 27 × 22 × 26 cm high) with a metal grid floor. To enable the rat to distinguish easily the transparent box from the black one, the floors of the transparent and black boxes were covered with white plastic mesh and black frosting Plexiglas, respectively. Each box could be divided by a sliding door (10 × 26 cm high). The place conditioning paradigm was performed with a minor modification (Nagai *et al.* 2004; Nakajima *et al.* 2004). In the pre-conditioning test, the sliding door was opened and the rat was allowed to move freely between both boxes for 15 min once a day for 3 days. On the third day of the pre-conditioning test, we measured pre-value by using a Scanet SV-10 LD (Tokyo Sangyo Co Ltd, Toyama, Japan). On days 4, 6, and 8, a rat was given METH at 2 mg/kg and put in its

non-preferred side for 30 min. On days 5, 7, and 9, the rat was given saline and placed opposite the drug-conditioning side. In the post-conditioning test, the sliding door was opened, and we measured post-value. Place conditioning behaviors were expressed as [(post-conditioning preference)-(pre-conditioning preference)].

TIMP-2 antisense oligonucleotide treatment

Rats were anesthetized with pentobarbital (40 mg/kg, i.p.) and placed in a stereotaxic apparatus. The infusion cannula was connected to a miniosmotic pump (total capacity: 100 μL, Alzet 1007D, Alza, Palo Alto, CA, USA), which was filled with TIMP-2 antisense (TIMP-AS) or scramble oligonucleotides (TIMP-SC), and was implanted into the right ventricle [anteroposterior (AP) -0.8, mediolateral (ML) +1.5 from bregma, dorsoventral (DV) -4.0 from the skull, according to the atlas of Paxinos and Watson (1982)]. Phosphothioate oligonucleotides were custom-synthesized at Nisshinbo Biotechnology (Tokyo, Japan) and dissolved in artificial cerebrospinal fluid (aCSF; 147 mmol/L NaCl, 3 mmol/L KCl, 1.2 mmol/L $CaCl_2$, and 1.0 mmol/L $MgCl_2$, pH 7.2). The sequences of TIMP-AS and TIMP-SC were 5′-CC GCGGCGCCCAT-3′ and 5′-AGCGCGCGCCGTGCC-3′, respectively. The TIMP-AS and TIMP-SC were continuously infused into the cerebral ventricle at a dose of 3.6 nmol/day. The infusion of the oligonucleotide was maintained for 5 days (flow rate, 0.5 μL/h). One day after the start of oligonucleotide infusion, the rats (n = 7–11) were subjected to METH treatment for sensitization.

MMP inhibitor treatment

Doxycycline is a second-generation tetracycline antibiotic with an inhibitory effect on MMP (Uitto *et al.* 1994; Smith *et al.* 1996). Doxycycline at 10–100 μg/mL inhibits MMP-9 activity in brain tissue *in vitro* study (Hashimoto *et al.* 2005). MMP-2/-9 inhibitor III is a potent inhibitor of MMP-2 (IC_{50}=10 μmol/L) according to the manufacturer (Koivunen *et al.* 1999).

Rats were anesthetized with pentobarbital and placed in a stereotaxic apparatus. The infusion cannula was connected to a miniosmotic pump (total capacity: 200 μL, Alzet 2002; Alza, Palo Alto, CA, USA), which was filled with doxycycline (n = 18) (60 μg/12 μL/day) or MMP-2/-9 inhibitor III (n = 18) (2.4 μg/12 μL/day, Merck kGaA, Darmstadt, Germany), and was implanted into the right ventricle (AP −0.8, ML +1.5 from bregma, DV −4 from the skull) for CPP. MMP-2/-9 inhibitor III was dissolved in 2% DMSO in saline. Alternatively, the infusion cannula was connected to a miniosmotic pump (total capacity: 100 μL, Alzet 1007D), which was filled with aCSF (n = 10) or doxycycline (n = 10) (0.06 μg/12 μL/day), and was bilaterally implanted into the frontal cortex (AP +2.5, ML ± 0.6 from bregma, DV -3.0 from the skull). One day after the start of doxycycline infusion, the rats were subjected to METH treatment for sensitization.

Quantitative analysis of TIMP-2 mRNA by real-time PCR

After a final administration of METH, rats were intracardially perfused with cold saline and then decapitated as described (n = 4–10) (Asahi *et al.* 2001; Lee *et al.* 2004). Various regions of the brain including the Fc, NAc, striatum (St) and ventral tegmental area (VTA), were dissected from freshly perfused brains and immediately frozen and stored at −80°C until assayed. All dissection was made using brain matrix (NeuroScience Idea, Osaka, Japan) and based on the atlas of Paxinos and Watson (1982).

The sequences of forward and reverse primers for the rat TIMP-2 were 5′-GCAAGATGCACATTACCCTCTGT-3′ and 5′-CCATCT GGTACCTGTGGTTTAGG-3′, respectively, giving rise to a 92-bp PCR product. cDNA was synthesized from total RNA by reverse transcriptase using a superscript II kit. The cDNA was synthesized from 1 μg of total RNA for TIMP-2. For standardization of the quantitation, glyceraldehde-3-phosphate dehydrogenase was amplified simultaneously. The change in reporter fluorescence from each reaction tube was monitored with an ABI PRISM 7700 Sequence Detection System (Applied Biosystems, Foster City, CA, USA).

Gel zymography

Sample preparation was made as described previously (n = 4) (Zhang and Gottschall 1997; Mizoguchi *et al.* 2007). Briefly, brain tissues were homogenized in lysis buffer [50 mmol/L Tris–HCl, 150 mmol/L NaCl, 5 mmol/L $CaCl_2$, 0.05% Brij35, and 0.02% NaN_3, pH 7.6] with 1% TritonX-100 and centrifuged at 12 000 *g* for 10 min to pellet insoluble material. The protein concentration in the supernatant was determined using a Protein Assay Rapid Kit (Bio-Rad, Osaka, Japan). The supernatant was incubated with gelatin-sepharose 4B (GE Healthcare Bio-Science Corp., Piscataway, NJ, USA) that had previously washed three times with the lysis buffer, with constant shaking, for 24 h at 4°C. After centrifugation at 500 *g* for 2 min, the pellet was resuspended in 500 μL of the lysis buffer and washed three times. The pellet was resuspended in 150 μL of lysis buffer containing 10% dimethyl sulfoxide and shaken for 2 h, and used for assaying gelatinase activity of MMP-2 and MMP-9.

The samples were subjected to electrophoresis in 10% SDS-polyacrylamide gel electrophoresis (SDS-PAGE) containing 0.1% gelatin under non-reducing conditions. Gels were washed twice for 30 min in 2.5% Triton X-100 to remove SDS, washed for 30 min in incubation buffer [50 mmol/L Tris–HCl, 5 mmol/L $CaCl_2$, 2 μmol/L $ZnCl_2$, 200 mmol/L NaCl, and 0.02% Briji 35, pH 7.4] at 25 ± 2°C, and further incubated for 24 h in the same buffer at 37°C. Gels were then stained for 3 h in Coomassie blue (1% Coomassie brilliant blue G-250, 30% methanol, 10% acetic acid) and destained in 40% methanol/7% acetic acid until clear bands of gelatinolysis appeared on a dark background. Total activity including pro-MMP was analyzed with the ATTO Densitograph Software Library Lane Analyzer (Atto Instruments, Tokyo, Japan).

Western blotting

Brain tissues were homogenized in lysis buffer [20 mmol/L Tris–HCl, 100 mmol/L NaCl, 1 mmol/L $CaCl_2$, and 0.005% Brij35, p H7.4], and microwaved for 15 s according to the protocol for immunoblotting with monoclonal antibodies (n = 5). The homogenate was centrifuged at 13 000 *g* for 30 min to pellet insoluble material. The protein concentration in the supernatant was determined using a Protein Assay Rapid Kit (Bio-Rad Laboratories, Hercules, CA, USA). The sample was boiled in 2× sample buffer [0.25% bromophenol blue/12% 2-mercaptothanol/20% glycerol/4% SDS/0.1 mol/L Tris–HCl, pH 6.8] and electrophoresed by SDS-polyacrylamide gel electrophoresis (SDS-PAGE) on a 4.75% stacking gel and 10 or 13% separating gel, and then transferred electrophoretically to a polyvinylidene difluoride membrane (Millipore, Bedford, MA, USA). The same concentration (20–40 μg) of protein per lane was loaded for all western blotting. The band intensities of the film were analyzed by densitometry. The amount of TIMP-2 was calculated versus the

amount of β-actin protein. The primary polyclonal rabbit or goat antibodies used in the present study were anti-TIMP-2 (1 : 1000; Chemicon, Temecula, CA, USA) and β-actin (1 : 2000; Santa Cruz Biotechnology, Santa Cruz, CA, USA). The secondary antibodies, used at a 1 : 2000 or 1 : 5000 dilution, were horseradish peroxidase-linked anti-rabbit or anti-goat IgG (Kirkegaard & Perry Laboratories, Inc., Gaithersburg, MD, USA). Immunoreactive materials on the membrane were detected using ECL western blotting detection reagents (Amersham Pharmacia Biotech, Arlington Heights, IL, USA) and exposed to X-ray film. The band intensities of the film were analyzed by densitometry.

Double immunostaining

Polyclonal rabbit anti-TIMP-2 antibody (1 : 250; Chemicon), monoclonal mouse anti-neuron-specific nuclear antigen (NeuN) antibody (1 : 200; Chemicon) and anti-glial fibrillary acidic protein (GFAP) antibody (1 : 200; Chemicon) served as primary antibodies. Affinity-purified FITC-conjugated goat anti-rabbit IgG and rhodamine-conjugated goat anti-mouse IgG served as secondary antibodies. Samples were observed with AXIOVISION 3.0 systems (Carl Zeiss, Jene, Germany).

In vivo microdialysis

Rats were anesthetized with sodium pentobarbital before stereotaxic implantation of a guide cannula into the left Fc (AP +2.5, ML +0.8 from the bregma, DV -2 from the skull) or NAc (AP +1.6, ML +1.0 from the bregma, DV -7 from the skull). When the infusion cannula for doxycycline treatment was bilaterally implanted into the Fc (n = 7), a guide cannula was implanted into the NAc (20° from AP +1.6, ML +1.5 from the bregma, and DV −7.5 from the skull). One day after the surgery, a dialysis probe (AI-4–2 or AI-8–1; 1- or 2-membrane length, EICOM, Kyoto, Japan) was inserted though a guide cannula and perfused with aCSF (147 mmol/L NaCl/ 4 mmol/L KCl/ 2.3 mmol/L $CaCl_2$) at a flow rate of 1.2 μL/min. Outflow fractions were collected every 20 min. After the collection of three baseline fractions, rats were treated with METH (2 mg/kg, s.c.). Dopamine levels in the dialysates were analyzed as described (Nagai *et al.* 2004).

[^{35}S] GTPγS binding assay

For the membrane preparation, rats were repeatedly treated with METH at 2 mg/kg for 5 days. The TIMP-AS- (n = 8–11) and doxycycline- (n = 5–7) infused rats were treated with METH at 2 mg/kg for 3 days and 5 days, respectively. Wild-type mice, MMP-2-(−/−) mice (n = 6–7) and MMP-9-(−/−) mice (n = 5) were treated with METH at a dose of 1 mg/kg for 7 days. The Fc was dissected out and immediately frozen and stored at −80°C until assayed. All dissection was made using brain matrix and based on the atlas of Paxinos and Watson (1982) for rat and Frankin and Paxinos (1997) for mouse.

The animals were killed 2 h after the last treatment, and the Fc was homogenized in 20 volumes (w/v) of buffer containing 50 mmol/L Tris–HCl, 5 mmol/L $MgCl_2$ and 1 mmol/L EGTA, pH 7.4. The homogenate was centrifuged at 48 000 g for 10 min at 4°C and the pellet was resuspended in the assay buffer containing 50 mmol/L Tris–HCl, 5 mmol/L $MgCl_2$, 1 mmol/L EGTA, and 100 mmol/L NaCl (pH 7.4). The [^{35}S]GTPγS binding assay was performed according to the procedures described by Bowers *et al.* (2004) with a minor modification. Briefly, the membrane homogenate (10 μg protein) was incubated at 25°C for 2 h in 1 mL of the assay buffer with various concentrations of the agonists, 0.5 U of adenosine deaminase, 20 μmol/L guanosine-5′-diphosphate (GDP) and 100 pmol/L [^{35}S] GTPγS (Amersham Biosciences, Arlington Heights, IL, USA). The reaction was terminated by rapid filtration using Whatman GF/B glass filters. The filters were washed three times and then transferred to scintillation counting vials containing tissue solubilizer (Soluene-350, Perkin-Elmer Life Sciences, Japan) and scintillation cocktail (Hionic Fluor, Perkin-Elmer Life Sciences, Japan). The radioactivity in the samples was determined with a liquid scintillation analyzer. Non-specific binding was measured in the presence of 10 μmol/L of unlabeled GTPγS. The data are expressed as the percentage of basal [^{35}S]GTPγS binding measured in the presence of GDP and absence of agonist.

To investigate the effect of *in vitro* treatment with exogenous MMP-2 and TIMP-2 on [^{35}S]GTPγS binding, brain homogenates (100 μg) were incubated with vehicle (5 mmol/L Tris–HCl, 0.1 mmol/L $CaCl_2$, and 0.005% Brij35, pH 7.5) or purified human MMP-2 (Chemicon) at a dose of 0.4 μg in the activation buffer (50 mmol/L Tris–HCl, 100 mmol/L NaCl, 10 mmol/L $CaCl_2$, 0.05% Brij35 and 0.02% NaN_3, pH 7.4) in the presence or absence of 1 mmol/L EGTA at 37°C for 60 min (n = 5–7). Alternatively, brain homogenates (100 μg protein) were incubated with vehicle (PBS buffer) or recombinant human TIMP-2 protein (Daiichi FineChem., Takaoka, Japan) at a dose of 1 μg in the assay buffer without EGTA at 4°C for 120 min (n = 5–7). The sample was centrifuged at 48 000 g at 4°C for 10 min and the pellet was resuspended in the assay buffer with 1 mmol/L EGTA for [^{35}S]GTPγS binding.

Statistical analyses

Results were expressed as the means ± SE. The significance of differences was determined by one-way ANOVA, followed by the Student–Newman–Keuls test or by repeated ANOVA, followed by Sheffe's test for multi-group comparisons. Student's t-test was used for two-group comparison.

Results

METH increases TIMP-2 expression in the brain

In a DNA microarray screening, we have found that repeated METH treatment induces the gene expression of extracellular proteinase-related proteins, such as tissue plasminogen activator and TIMP-2 in the rat brain (Yamada *et al.* 2005). Additionally, repeated but not acute METH treatment induces MMP-2 and MMP-9 expression in neurons and glial cells in the Fc and NAc (Mizoguchi *et al.* 2007). Therefore, to further clarify the MMP/TIMP system on METH-induced behavioral sensitization and dependence, we examined whether single and repeated METH treatment altered the expression of TIMP-2 mRNA in the brain of rats, using a real-time reverse transcription-PCR method. Acute METH treatment at a dose of 2 mg/kg did not change TIMP-2 gene expression in any regions examined. When METH treatment was repeated for 5 days, METH-induced hyperactivity was significantly potentiated (sensitization, Fig. 1a),

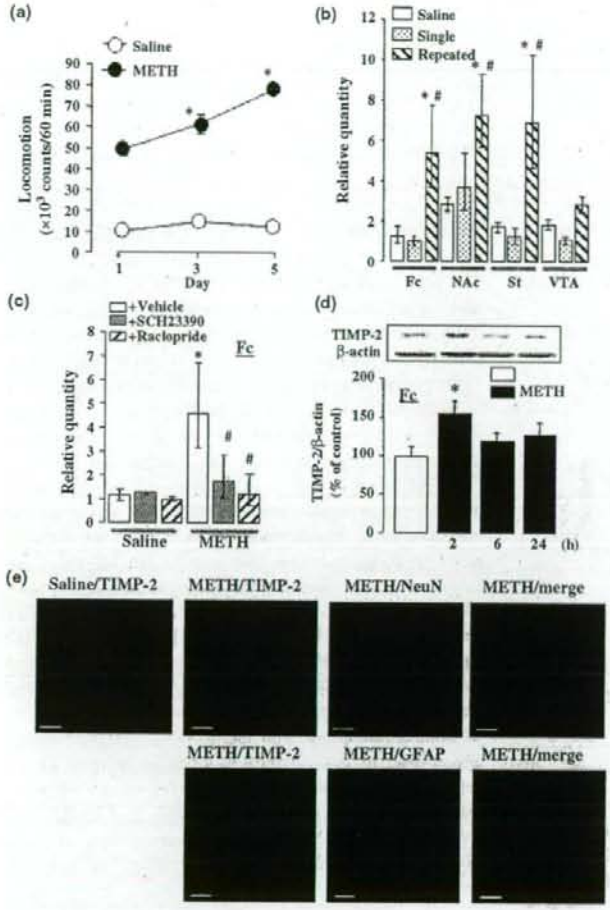

Fig. 1 METH-induced behavioral sensitization in rats (a): METH was administered at a dose of 2 mg/kg for 5 days. Values are means ± SE (n = 7–8). *p < 0.05 versus METH (day 1). Changes in the expression of TIMP-2 mRNA in the brain after METH treatment (b): rats were killed 2 h after a single or repeated METH treatment (2 mg/kg, s.c. for 5 days). Values are means ± SE (n = 5–10). *p < 0.05 versus saline, # p < 0.05 versus single METH treatment. The effects of the dopamine D1 receptor antagonist SCH23390 and D2 receptor antagonist raclopride on the METH-induced increase in TIMP-2 mRNA expression in the Fc (c): SCH23390 (0.1 mg/kg) or raclopride (2 mg/kg) was administered i.p 30 min before daily METH (2 mg/kg) treatment for 5 days. Values are means ± SE (n = 4–6 for C). *p < 0.05 versus saline+vehicle, #p < 0.05 versus METH+vehicle. Changes in the expression of TIMP-2 protein in the Fc after repeated METH treatment (d): Rats were given METH at a dose of 2 mg/kg for 5 days and killed 2, 6 or 24 h after the final administration. Control rats were given saline. *p < 0.05 versus control group. Values are means ± SE (n = 6–7). Double immunostaining for TIMP-2 and NeuN or GFAP reveals TIMP-2 expression in neurons of the Fc (e): rats were killed 2 h after repeated administration of METH (2 mg/kg, for 5 days). Scale bar: 20 μm.

and TIMP-2 mRNA levels were significantly elevated to 200–500% of the control level in the Fc ($F_{(2,17)}$ = 3.89, p < 0.05), NAc ($F_{(2,26)}$ = 5.96, p < 0.05) and St ($F_{(2,16)}$ = 4.25, p < 0.05), but not the VTA (Fig. 1b). Because it is well known that dopaminergic neuronal system is involved primarily in the pharmacological effects of METH, we examined whether the METH-induced increase in TIMP-2 mRNA levels is mediated by the activation of dopaminergic neurotransmission. The METH-induced increase in TIMP-2 mRNA expression was significantly and completely inhibited by pretreatment with either the dopamine D1 receptor antagonist SCH23390 ($F_{(3,16)}$ = 4.50, p < 0.05 in the Fc) or the dopamine D2 receptor antagonist raclopride ($F_{(3,37)}$ = 5.48, p < 0.05 in the Fc), suggesting that METH-induced gene expression of TIMP-2 in the Fc is attributable to dopamine D1 and D2 receptor activation (Fig. 1c). We also investigated TIMP-2 protein expression in the Fc by western blotting (Fig. 1d) and immunohistochemistry (Fig. 1e). Repeated METH treatment increased TIMP-2 protein expression transiently in the Fc (Fig. 1d, $F_{(3,23)}$ = 3.26, p < 0.05). In addition, to determine the cell types in which the expression of TIMP-2 is induced by repeated METH treatment, double immunostaining for TIMP-2 with NeuN, a neuronal marker, or GFAP, a glial marker, was performed. The findings indicated the co-localization of TIMP-2 immunoreactivity with NeuN, suggesting the neuronal localization of TIMP-2 in th Fc (Fig. 1e).

Role of TIMP-2 in METH-induced sensitization

To study the role of TIMP-2 in METH-induced behavioral sensitization, an antisense oligonucleotide strategy was used to inhibit TIMP-2 in the brain. TIMP-AS or TIMP-SC was continuously infused in the lateral ventricle. Acute METH

treatment induced hyperlocomotion and the METH-induced hyperlocomotion was augmented by repeated METH treatment in the aCSF-injected control group. Neither TIMP-AS nor TIMP-SC affected spontaneous locomotor activity and the acute METH-induced hyperlocomotion. However, TIMP-AS treatment accelerated the development of the sensitization, while TIMP-SC had no effect: TIMP-AS-treated animals showed a marked potentiation of METH-induced hyperlocomotion as early as the third day of the treatment (Fig. 2a, $F_{(5,46)} = 36.7$, $p < 0.05$ by one-way ANOVA). The increase in TIMP-2 protein levels evoked by repeated METH treatment in the Fc was significantly abolished by TIMP-AS although TIMP-SC had little effect (Fig. 2b, $F_{(5,24)} = 4.52$, $p < 0.05$ by one-way ANOVA). Neither TIMP-AS nor TIMP-SC affected TIMP-2 protein levels in saline-treated group. These results suggest that TIMP-2 is involved in the development of the behavioral sensitization induced by repeated METH treatment.

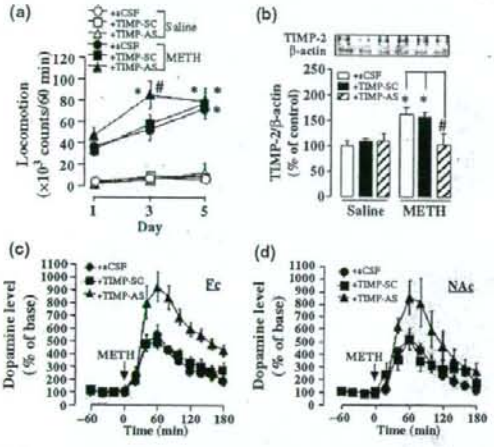

Fig. 2 Effects of TIMP-2 antisense oligonucleotide on repeated METH-induced behavioral sensitization (a), TIMP-2 protein expression in the Fc (b) and increased extracellular dopamine levels in Fc (c) and NAc (d). Rats were given saline or METH at a dose of 2 mg/kg for 5 days, and locomotor activity was measured on days 1, 3 and 5 (a): an osmotic minipump was used to deliver a continuous infusion of TIMP-AS (3.6 nmol/12 μL/day), TIMP-SC (3.6 nmol/12 μL/day) or aCSF into the right ventricle. Values are the means ± SE (n = 7–11). *$p < 0.05$ versus day 1, #$p < 0.05$ versus METH+aCSF, and METH+TIMP-SC. Rats were killed 2 h after saline or METH treatment on day 3 (b): values are the means ± SE (n = 5). *$p < 0.05$ versus saline+aCSF, #$p < 0.05$ versus METH+aCSF, and METH+TIMP-SC. Rats were given METH at a dose of 2 mg/kg for 3 days (c) and (d): On day 3, dopamine release was measured for 3 h after the administration of METH. Basal extracellular dopamine levels in Fc were 0.23 ± 0.03 nmol/L, 0.18 ± 0.04 nmol/L and 0.16 ± 0.04 nmol/L for aCSF-, TIMP-SC- and TIMP-AS-treated groups, respectively, and 0.44 ± 0.07 nmol/L, 0.44 ± 0.05 nmol/L and 0.62 ± 0.07 nmol/L in the NAc of aCSF-, TIMP-SC- and TIMP-AS-treated groups, respectively. Values are means ± SE (n = 5–7). In the TIMP-AS-treated group, the METH-induced increase in extracellular dopamine levels was significantly potentiated compared with the aCSF- or TIMP-SC-treated group in Fc and NAc ($F_{(2,13)}$=11.0; $p < 0.05$ by repeated ANOVA, and $p < 0.05$ by *post hoc*, $F_{(2,12)}$=4.13; $p < 0.05$ by repeated ANOVA, and $p < 0.05$ by *post hoc*). Fc: frontal cortex, NAc: nucleus accumbens.

Effects of TIMP-AS on METH-induced increase in extracellular dopamine levels in the Fc and NAc

The pharmacological effects of METH are linked to its capacity to elevate extracellular dopamine levels in the brain through redistribution of dopamine from synaptic vesicles to the cytosol and promotion of reverse transport (Sulzer *et al.* 1995; Nakajima *et al.* 2004). Sensitization is related to the extracellular dopamine level in the NAc, which is regulated by the excitatory input from the Fc (Beyer and Steketee 2002). Accordingly, to explore the mechanisms by which TIMP-AS strengthened the METH-induced sensitization on day 3, we examined the effects of TIMP-AS on the METH-induced increase in extracellular dopamine levels in the Fc and NAc, by using a microdialysis technique. METH caused a marked increase in extracellular dopamine levels in the Fc of the aCSF-treated group on the third day (Fig. 2c). Peak extracellular dopamine was increased by METH treatment to approximately 600% of the baseline level in the aCSF-treated group. In the TIMP-AS-treated group, the METH-induced increase in extracellular dopamine levels was significantly potentiated compared with the aCSF- or TIMP-SC-treated group (Fig. 2c, $F_{(2,13)} = 11.0$, $p < 0.05$ by repeated ANOVA, and $p < 0.05$ by *post hoc*). Similar alterations of the METH-induced increase in extracellular dopamine levels were evident in the NAc of TIMP-AS-treated rats (Fig. 2d, $F_{(2,12)} = 4.13$, $p < 0.05$ by repeated ANOVA, and $p < 0.05$ by *post hoc*).

Role of MMP in METH-induced sensitization in the rat

To study the role of MMP in the Fc in behavioral responses to METH, we investigated the effect of an MMP-2/-9 inhibitor, doxycycline. It has been demonstrated that doxycycline binds directly to Zn^{2+} or Ca^{2+} associated with the enzyme, and blocks the active site or induces conformational changes that render the proenzyme susceptible to fragmentation during activation (Smith *et al.* 1996). It also inhibits the transcription of MMP mRNA (Uitto *et al.* 1994). Recently, it has been reported that doxycycline prevents the activation of pro-MMP-2 by MMP-14 *in vivo* (Strongin *et al.* 1995).

In the present study, doxycycline (0.06 μg/12 μL/day) or aCSF was continuously infused into Fc for 7 days. Acute METH treatment induced hyperlocomotion and the METH-induced hyperlocomotion was augmented by repeated METH treatment in the aCSF-injected control group. Doxycycline did not affect spontaneous locomotor activity or

acute METH-induced hyperlocomotion, but significantly inhibited the development of behavioral sensitization on day 5 (Fig. 3a, $F_{(3,15)} = 54.9$, $p < 0.05$ by one-way ANOVA). The increase in MMP-2 and MMP-9 activity after challenge administration of METH (1 mg/kg) on day 7 was significantly abolished in the Fc and NAc of doxycycline-treated rats (Fig. 3b, $F_{(4,15)} = 8.29$, $p < 0.05$ by one-way ANOVA; and Fig. 3c, $F_{(4,15)}$=5.62, $p < 0.05$ by one-way ANOVA), although the inhibitor had little effect on MMP-2 activity in the saline-treated control.

Effect of doxycycline infusion into the Fc on the METH-induced increase in extracellular dopamine levels in the NAc

Because doxycycline prevented the development of METH-induced behavioral sensitization, we compared the extracellular dopamine levels in the NAc after METH treatment on day 5 in the doxycycline-injected rats with those in the aCSF-treated control animals. Repeated METH treatment for 5 days increased the peak extracellular dopamine levels to about 800–900% of the basal levels in the NAc, which may be associated with behavioral sensitization (Sulzer *et al.* 1995; Nakajima *et al.* 2004) (Fig. 3b). Continuous infusion of doxycycline at 0.06 μg/day into the Fc significantly reduced the METH-induced increase in the extracellular dopamine levels on day 5 (Fig. 3d, $F_{(1,12)} = 5.01$, $p < 0.05$ by repeated ANOVA, and $p < 0.05$ by *post hoc*). From the results of the infusion of doxycycline into the Fc, it is suggested that MMP, possibly MMP-2 and/or MMP-9, in the Fc plays an important role in the METH-induced dopamine release in the NAc.

Next, the role of MMP in the rewarding effects of METH was examined in a CPP paradigm, in which animals learned to associate the environment paired with drug exposure. CPP is therefore considered a measure of the rewarding properties of drugs of abuse. When doxycycline or MMP-2/-9 inhibitor III was continuously infused into the right ventricle of rats, METH-induced CPP was significantly attenuated (Fig. 3e, $F_{(3,33)} = 5.77$, $p < 0.05$ by one-way ANOVA; Fig. 3f, $F_{(3,33)} = 6.48$, $p < 0.05$ by one-way ANOVA), although these inhibitors had no effect in saline-treated animals. These results suggest that MMP, especially MMP-2 and MMP-9, is involved in METH reward.

Regulation of dopamine receptor-stimulated G protein signaling by the MMP/TIMP system

As shown in Figs 2 and 3, over-expression of the MMP/TIMP system in the Fc may play a crucial role in the development of METH-induced sensitization. Behavioral sensitization to METH could also be associated with alterations in the responsiveness of post-synaptic dopamine receptors which belong to G protein-coupled receptors. In fact, G protein signaling in the Fc plays a crucial role in a potential pathological change contributing to cocaine sensitization and drug seeking (Bowers *et al.* 2004). The reduced signaling via Gi-coupled receptors may be an important neuroadaptation in cocaine addiction (Goldstein and Volkow 2002). Therefore, we focused on the dopaminergic signaling via the dopamine D1 and D2 receptors in the Fc. To assess potential changes in dopamine receptor-stimulated G protein signaling, we performed a [^{35}S]GTP γS binding assay. The ability of the dopamine D1 receptor agonist SKF81297 (0.01–0.1 mmol/L) and D2 receptor agonist quinpirole (0.5–1 mmol/L), to stimulate the binding of [^{35}S]GTP γS to Gα proteins in membranes of the Fc in METH-treated rats was compared with that in the saline-treated control group (Fig. 4a). Repeated METH treatment for 5 days reduced the [^{35}S]GTP γS binding stimulated by SKF81297 or quinpirole in membrane of the Fc, indicating a reduction of both dopamine D1 and D2 receptor-stimulated G protein signaling in the Fc (Fig. 4a, $p < 0.05$ by *t*-test). Interestingly, TIMP-AS treatment, which potentiated METH-induced behavioral sensitization and dopamine release on day 3 of the repeated METH treatment (Fig. 2), was accompanied by potentiation of the reduction of [^{35}S]GTPγS binding stimulated by quinpirole ($F_{(5,49)} = 5.00$, $p < 0.05$ by one-way ANOVA) although TIMP-SC had no effect (Fig. 4c). Neither TIMP-AS or TIMP-SC had effects on SKF81297-stimulated [^{35}S]GTPγS binding (Fig. 4b). In contrast, doxycycline treatment, which inhibited METH-induced behavioral sensitization and dopamine release on day 5 of the repeated METH treatment (Fig. 3a), was accompanied by blockade of the reduction of [^{35}S]GTPγS binding stimulated by quinpirole (Fig. 4e, $F_{(3,23)} = 3.03$, $p < 0.05$ by one-way ANOVA at 10^{-3} mol/L).

To further confirm the role of the MMP/TIMP system in the regulation of dopamine receptor-mediated G protein signaling in the Fc, the effects of *in vitro* treatment with purified human MMP-2 and recombinant human TIMP-2 protein on SKF81297- or quinpirole-stimulated [^{35}S]GTPγS binding were determined (Fig. 5). Purified human MMP-2 treatment at 37°C for 60 min *in vitro* significantly reduced the quinpirole-stimulated [^{35}S]GTPγS binding (Fig. 5b, $F_{(2,15)} = 5.51$, $p < 0.05$; $F_{(4,24)} = 4.02$, $p < 0.05$ by one-way ANOVA), without affecting the binding stimulated by SKF81297 (Fig. 5a). Co-treatment with EGTA (1 mmol/L) blocked the reduction of [^{35}S]GTPγS binding induced by purified human MMP-2 ($p < 0.05$ by *post hoc*). In contrast, the *in vitro* TIMP-2 treatment at 4°C for 120 min increased the quinpirole-stimulated [^{35}S]GTPγS binding (Fig. 5d, $F_{(2,18)} = 3.87$, $p < 0.05$; $F_{(2,17)} = 3.98$, $p < 0.05$ by one-way ANOVA), but had no effect on the SKF81297-stimulated binding (Fig. 5c). Thus, it is plausible that repeated METH treatment induces over-expression of MMP-2, MMP-9 and TIMP-2, leading to an increase in net MMP activity, which results in the potentiation of METH-induced dopamine release in the NAc as well as down-regulation of dopamine D2 receptor-mediated G protein signaling in the Fc.

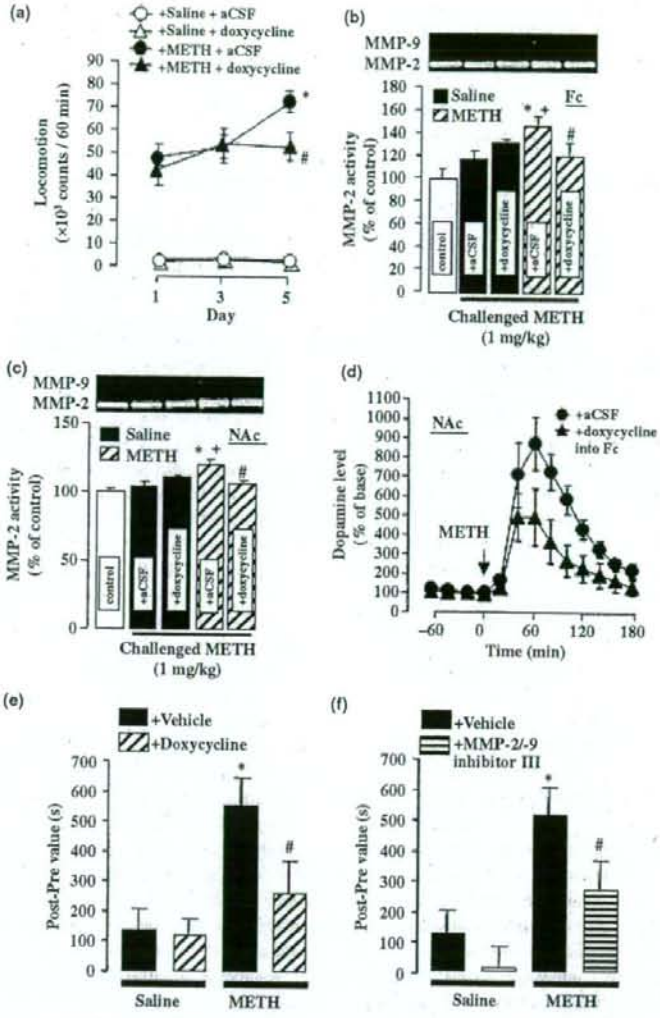

Fig. 3 Effect of continuous infusion of MMP inhibitor, doxycycline into Fc on repeated METH-induced behavioral sensitization (a), MMP-2 activity in Fc (b) and NAc (c), and dopamine release in NAc (d). (a): Rats were given saline or METH at a dose of 2 mg/kg for 5 days, and locomotor activity was measured on days 1, 3 and 5. An osmotic minipump was used to deliver a continuous infusion of doxycycline (0.06 μg/12 μL/day) or aCSF into the Fc for 7 days. Values are the means ± SE (n = 4–6). *p < 0.05 versus day 1, #p < 0.05 versus METH+aCSF. (b) and (c): Rats were given saline or METH at a dose of 2 mg/kg for 5 days. On day 7, rats were given METH at the challenge dose of 1 mg/kg and killed 2 h after the administration. Control rats were given saline. An osmotic minipump was used to deliver a continuous infusion of doxycycline (0.06 μg/12 μL/day) or aCSF into the Fc for 7 days. Values are the means ± SE (n = 4). *p < 0.05 versus control, +p < 0.05 versus saline+vehicle and # p < 0.05 versus METH+vehicle. (d): rats were given METH at a dose of 2 mg/kg for 5 days. Doxycycline (0.06 μg/12ul/day) was continuously infused by the osmotic minipump into the Fc. On day 5, dopamine release was measured for 3 h after the administration of METH in the NAc. Basal extracellular dopamine levels were 0.29 ± 0.07 nmol/L for the control and 0.18 ± 0.05 nmol/L for the doxycycline-infused group. Values are the means ± SE (n = 7). Continuous infusion of doxycycline at 0.06 μg/day into Fc significantly reduced the METH-induced increase in the extracellular dopamine levels on day 5 ($F_{(1,12)}$=5.01; p < 0.05 by repeated ANOVA, and p < 0.05 by *post hoc*). Effects of doxycycline (e) and MMP-2/-9 inhibitor III (f) on the rewarding effects of METH. Rats were trained for CPP to METH (2 mg/kg). Doxycycline or MMP-2/-9 inhibitor III was continuously infused into the right ventricle. Values are the means ± SE (n = 9–10). *p < 0.05 versus saline+vehicle. #p < 0.05 versus METH+vehicle. Fc: frontal cortex, NAc: nucleus accumbens.

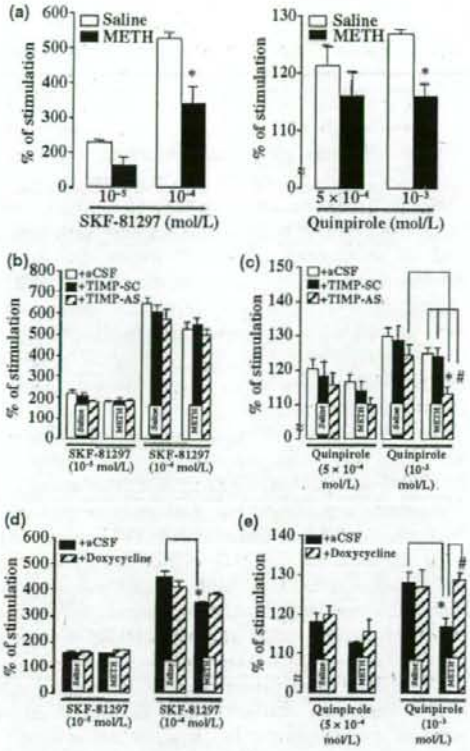

Fig. 4 Effects of repeated METH treatment on dopamine D1 agonist SKF81297- and D2 agonist quinpirole-stimulated [^{35}S]GTPγS binding in membranes of the Fc (a). Rats were given saline or METH at a dose of 2 mg/kg for 5 days and killed 2 h after the final administration. Values are means ± SE (n = 4). *p < 0.05 versus saline. Effects of TIMP-AS on SKF81297- (b) and quinpirole-stimulated (c) [^{35}S]GTPγS binding in membranes of saline- and METH-treated rats. Rats were given saline or METH at 2 mg/kg for 5 days and killed 2 h after the final administration. aCSF, TIMP-AS or TIMP-SC was continuously infused into the cerebral ventricle. Values are mean ± SE (n = 8–11 for b and c). *p < 0.05 versus saline+TIMP-AS. #p < 0.05 versus METH+TIMP-SC. Effects of doxycycline on SKF81297-(d) and quinpirole-(e) stimulated [^{35}S]GTPγS binding in membranes of saline- and METH-treated rats. Rats were given saline or METH at a dose of 2 mg/kg for 5 days and killed 2 h after the final administration. CSF or doxycycline was continuously infused into the cerebral ventricle. Values are means ± SE (n = 5–7 for d; n = 7 for e). *p < 0.05 versus saline+vehicle. #p < 0.05 versus METH+vehicle.

Reduction of dopamine receptor-stimulated G protein signaling in MMP-2-(−/−) and MMP-9-(−/−) mice

Previously, we have demonstrated that MMP-2-(−/−) and MMP-9-(−/−) mice show reduced responses to METH in behavioral sensitization, CPP and dopamine release in the NAc. TIMP-2 is not a specific inhibitor of MMP-2 and

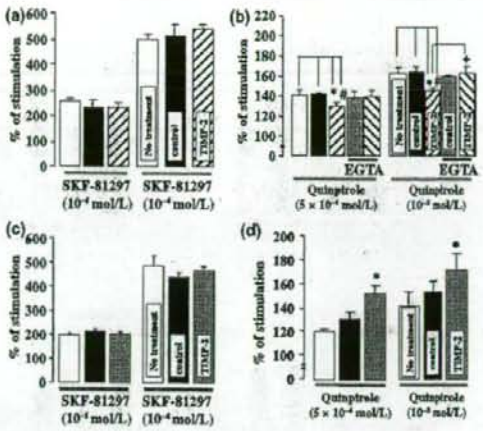

Fig. 5 Effects of *in vitro* treatment with purified human MMP-2 (a, b) or recombinant human TIMP-2 (c, d) on SKF81297- (a, c) and quinpirole-stimulated (b, d) [^{35}S]GTPγS binding in membranes of the Fc. Brain samples were incubated with activation buffer (control group) or purified human MMP-2 protein (MMP-2 group) in the presence or absence of 1 mmol/L EGTA at 37°C for 60 min. Alternatively, brain samples were incubated with activation buffer (control group) or recombinant human TIMP-2 protein (TIMP-2 group) for 120 min. Values are means ± SE (n = 5 for a; n = 5–7 for b; n = 5–6 for c; n = 6–7 for d). *p < 0.05 versus no treatment. #p < 0.05 versus control group. + p < 0.05 versus MMP-2 group.

tetracycline derivatives such as doxycycline inhibit most if not all of the MMPs that have been tested. Therefore, in addition to the pharmacological studies, we investigated a role of MMP-2 and MMP-9 in G protein signaling using MMP-2-(−/−) and MMP-9-(−/−) mice.

We observed no changes in SKF-81297 or quinpirole-stimulated [^{35}S]GTPγS binding between saline-treated wild-type and MMP-2-(−/−) or MMP-9-(−/−) mice, indicating no changes in dopamine D1 and D2 receptor activity in MMP-2-(−/−) and MMP-9-(−/−) mice (Fig. 6). Repeated METH treatment for 7 days reduced the [^{35}S]GTP γS binding stimulated by SKF81297, but not quinpirole, in membranes of the Fc of wild-type mice (Figs 6a and b, $F_{(3,16)} = 4.66$, $p < 0.05$ by one-way ANOVA for SKF-81297 at 10^{-5} mol/L; $F_{(3,16)} = 5.00$, $p < 0.05$ by one-way ANOVA for SKF-81297 at 10^{-4} mol/L). Such METH-induced reduction of [^{35}S]GTPγS binding stimulated by SKF81297 at 10^{-5} mol/L, but not 10^{-4} mol/L, was significantly attenuated in MMP-9-(−/−) mice (Fig. 6a). Repeated METH treatment-induced [^{35}S]GTPγS binding stimulated by quinpirole was increased in MMP-9-(−/−) mice compared with wild-type mice (Fig. 6b, $p < 0.05$ by t-test). On the other hand, in the MMP-2-(−/−) mice, repeated METH treatment failed to reduce the [^{35}S]GTP γS binding stimulated by SKF81297 significantly at 10^{-4} mol/L or quinpirole at 10^{-3} mol/L as

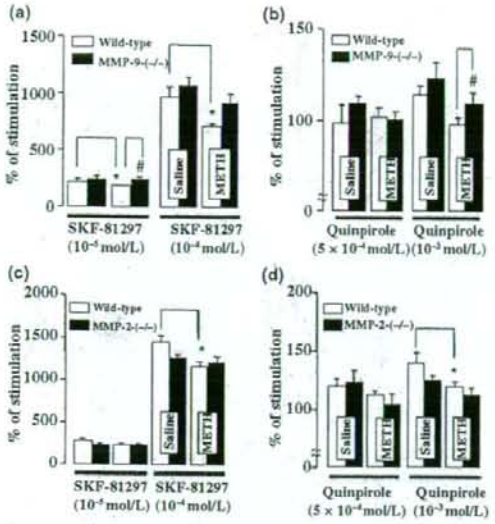

Fig. 6 Effects of repeated METH treatment on dopamine D1 agonist SKF81297- (a, c) and D2 agonist quinpirole-stimulated (b, d) [^{35}S]GTPγS binding in membranes of the Fc of MMP-9-(−/−) (a, b) and MMP-2-(−/−) (c, d) mice. Mice were given saline or METH at a dose of 1 mg/kg for 7 days and killed 2 h after the final administration. Values are means ± SE (n = 5 for A and B, n = 6–7 for c and d). *$p < 0.05$ versus saline-treated wild-type. *$p < 0.05$ versus saline-treated wild-type. #$p < 0.05$ versus METH-treated wild-type.

observed in wild-type mice, although there was no difference in [^{35}S]GTPγS binding stimulated by SKF81297 and quinpirole between two groups of mice (Fig. 6c, $F_{(3,24)} = 3.32$, $p < 0.05$ by one-way ANOVA at 10^{-4} mol/L; 6D, $F_{(3,21)} = 3.49$, $p < 0.05$ by one-way ANOVA at 10^{-3} mol/L). These results suggest that both mutant mice exhibit some resistance to the inhibitory effect of repeated METH treatment on dopamine receptor-mediated G protein signaling, which may be associated with the impairment in METH-induced behavioral sensitization and CPP, as well as METH-increased dopamine release in MMP-2-(−/−) and MMP-9-(−/−) mice (Mizoguchi *et al.* 2007).

Discussion

In the present study, we have demonstrated for the first time that repeated but not acute METH treatment leads to an increase in TIMP-2 expression in neurons in the Fc. The MMP inhibitor doxycycline prevented while TIMP-AS accelerated the development of the METH-induced behavioral sensitization. The net increase in MMP activity may be responsible at least in part for the development of METH-induced behavioral sensitization. Of note, MMP inhibitors also reduced the rewarding effect of METH. Further, we provided evidence that the MMP/TIMP system is involved in the regulation of METH-induced dopamine release as well as dopamine receptor-mediated G protein signaling. It is likely that MMP/TIMP system plays a role in METH-induced behavioral sensitization through the modulation of the function of plasma membrane protein such as dopamine receptors (The present study) and transporter (Mizoguchi *et al.* 2007). These results, together with the well known function of the MMP to degrade extracellular matrix proteins such as laminin and collagen IV, suggest that repeated METH-induced over-expression of the MMP-2, MMP-9 (Mizoguchi *et al.* 2007) and TIMP-2 (The present study) plays a crucial role in the structural and functional changes in the mesocorticolimbic dopamine system related to METH-induced behavioral sensitization and reward following repeated drug treatment.

Our data showed that repeated administration of METH led to behavioral sensitization which was accompanied by the induction TIMP-2 expression in the Fc. Additionally, we demonstrated that TIMP-2 was localized to neurons in the Fc. Previous study has revealed that MMP-2-like and TIMP-2-like immunoreactivities are found in cerebellar neurons but not glial cells (Vaillant *et al.* 1999). We have also shown that both MMP-2 and MMP-9 are highly expressed by neurons in the Fc of adult rat brain after repeated METH treatment (Mizoguchi *et al.* 2007). Taken together, it is suggested that the MMP/TIMP system is expressed by adult CNS neurons and the expression level and cellular localization may be regulated according to the developmental and/or functional status of neurons. In fact, MMP-7 disrupts dendritic spines in hippocampal neurons (Bilousova *et al.* 2006), and MMP-9 expression is regulated in the hippocampus by synaptic activity during dendritic remodeling (Zhang and Gottschall 1997), suggesting that MMP can influence the morphology of dendritic spines and hence synaptic stability. Although we do not directly examine the role of MMP/TIMP system in the METH-induced alterations of synaptic connectivity in the Fc, it is suspected that the expression of MMP/TIMP may take part in the structural and functional alteration in the brain following repeated exposure to METH.

The infusion of TIMP-AS into the ventricle exaggerated the behavioral sensitization induced by repeated METH treatment, while infusion of doxycycline and MMP-2/-9 inhibitor III inhibited the development of METH-induced behavioral sensitization and CPP. Consistent with the present findings, MMP-2-(−/−) and MMP-9-(−/−) mice exhibit the impairment of METH-induced behavioral sensitization and CPP (Mizoguchi *et al.* 2007). These findings suggest that METH-induced expression of the MMP/TIMP system in the brain plays a role in the development of METH-induced behavioral sensitization and reward, which may be associated with the METH-induced neuronal plasticity and remodeling. Indeed, cleavage of ECM induced by an imbalance of the MMP/TIMP ratio confers oncogenicity on the cell (Khokha *et al.* 1989), and excessive

proteolysis contributes to various brain pathologies (Rosenberg *et al.* 1992; Nakagawa *et al.* 1994). The inhibition of MMP alters functional and structural correlates of differentiation-induced sprouting such as remodeling in the dentate gyrus of the hippocampus (Reeves *et al.* 2003). In a behavioral study, MMP-9 knock-out mice display impairments in long-term potentiation and hippocampal-dependent memory in a fear-conditioning memory task (Nagy *et al.* 2006).

Behavioral changes induced by METH are linked to its capacity to elevate extracellular dopamine levels through the redistribution of dopamine from synaptic vesicles to the cytosol and promotion of reverse transport (Sulzer *et al.* 1995; Nakajima *et al.* 2004). In the present study, the behavioral effects of TIMP-AS and doxycycline on the METH-induced behavioral sensitization were correlated to changes in the METH-induced increase in extracellular dopamine levels in the NAc: TIMP-AS potentiated while doxycycline reduced the METH-induced dopamine release. These findings are in agreement with our previous report that microinjection of purified human MMP-2 directly into the NAc significantly potentiated the acute METH-induced increase in extracellular dopamine levels in the NAc and that METH-induced dopamine release in the NAc was significantly decreased in the MMP-2-(−/−) and MMP-9-(−/−) mice compared with the response in wild-type mice (Mizoguchi *et al.* 2007).

The sensitivity of dopamine receptors to endogenous and exogenous ligands is known to be an important parameter of dopamine-related functions in physiology and pathology. Reduced signaling via Gi-coupled receptors may be an important neuroadaptation in cocaine addiction (Goldstein and Volkow 2002). G protein signaling in the Fc plays a crucial role as a potential pathological change contributing to cocaine sensitization and drug seeking (Bowers *et al.* 2004). Therefore we investigated the role of the MMP/TIMP system in repeated METH treatment-induced changes in dopamine D1 and D2 receptor signaling. TIMP-AS treatment exaggerated the repeated METH-induced impairment of dopamine D2 receptor agonist-stimulated [^{35}S]GTPγS binding without affecting the impairment of dopamine D1 receptor agonist-stimulated binding. In contrast, doxycycline ameliorated the impairment of D2 receptor agonist-stimulated [^{35}S]GTPγS binding. Although the effects of TIMP-AS and MMP inhibitors used in this study are not specific to MMP-2 and MMP-9, we also demonstrated that MMP-2-(−/−) and MMP-9-(−/−) mice showed some resistance to the inhibitory effect of repeated METH treatment on dopamine D2 agonist-stimulated [^{35}S]GTPγS binding. Therefore, these results suggest that the changes in the dopamine receptor signaling induced by repeated METH treatment is attributable to METH-induced expression of the MMP/TIMP system. Indeed, *in vitro* treatment of membranes with purified human MMP-2 reduced while TIMP-2 treatment enhanced dopamine D2 receptor agonist-stimulated [^{35}S]GTPγS binding although they had no effect of the dopamine D1 receptor-stimulated binding. There were no differences in Gi protein levels between the TIMP-AS and TIMP-SC group, while METH treatment for 3 days decreased dopamine D2 receptor protein levels compared with the saline group (data not shown). Taken together, it is possible that the MMP-2 and MMP-9 are involved in the regulation of dopamine D2 receptor-mediated G protein signaling in the Fc. Because dopamine D2 receptors function as a feedback inhibition of dopamine release (Bowyer and Weiner 1987; Lindgren *et al.* 2001), their down-regulation may result in an enhancement of the METH-induced increase in extracelluar dopamine levels.

The molecular mechanisms by which the MMP/TIMP system regulates the METH-induced increase in extracelluar dopamine levels and the dopamine D2 receptor-mediated G protein signaling remain to be elucidated. It has been demonstrated that reverse activation of plasmalemmal dopamine transporter is involved in the METH-induced increase in extracellular dopamine levels. Degradation of ECM such as laminin by MMP may result in functional changes in plasmamembrane proteins such as dopamine transporter, dopamine receptors and G proteins. For instance, Freyer *et al.* (2004) have shown that ECM modulates Gi activity in human airway smooth muscle cells, and laminin in particular can activate Gi signaling. Laminin in the synaptic cleft localizes calcium channels to the sites of active zones (Sunderland *et al.* 2000) and induces a small but significant increase in calcium levels in ciliary ganglion neurons when applied in soluble form to the culture medium (Bixby *et al.* 1994). Alternatively, a recent study has indicated that cleavage of dystroglycan, which may be a target for MMP in the ECM, induces conformational changes that affect both pre- and postsynaptic elements (Kaczmarek *et al.* 2002). The deletion of neurexin, which is a pre-synaptic element for dystroglycan, in mice causes a severe reduction of Ca^{2+}-channel activity and a major decrease in evoked neurotransmitter release (Ushkaryov *et al.* 2002; Kattenstroth *et al.* 2004). Neurexin can also regulate the post-synaptic *N*-methyl-D-asparatate receptor function (Kattenstroth *et al.* 2004).

In conclusion, our findings suggest that the MMP-2, MMP-9 and TIMP-2 are involved in the rearrangement of the neural network in the mesocorticolimbic dopamine system, which plays a role in the development of behavioral sensitization to METH. It is speculated that the activation of the MMP/TIMP system in the Fc evoked by repeated METH treatment induces the cleavage of ECM such as laminin, resulting in an increase in the METH-induced dopamine release as well as a reduction in the efficacy of dopamine D2 receptor-mediated G protein signaling.

Acknowledgements

This study was supported in part by Grants-in Aid for Scientific Research (No. 18790052), the 21st Century COE Program from the

Ministry of Education, Culture, Sports, Science and Technology of Japan, Health Sciences Research from the Ministry of Health, Labour and Welfare of Japan, Special Coordination Funds for Promoting Science and Technology, Target-Oriented Brain Science Research Program from the Ministry of Education, Culture, Sports, Science and Technology of Japan, and an SRF Grant for Biomedical Research.

References

Asahi M., Wang X., Mori T., Sumii T., Jung J. C., Moskowitz M. A., Fini M. E. and Lo E. H. (2001) Effects of matrix metalloproteinases-9 gene knock-out on the proteolysis of blood-brain barrier and white matter components after cerebral ischemia. *J. Neurosci.* **21**, 7724–7732.

Berke J. and Hyman S. T. (2000) Addiction, dopamine, and the molecular mechanisms of memory. *Neuron* **25**, 515–532.

Beyer C. E. and Steketeé J. (2002) Cocaine sensitization: modulation by dopamine D2 receptors. *Cereb. Cortex* **12**, 526–535.

Bilousova T. V., Rusakov D. A., Ethell D. W. and Ethell I. M. (2006) Matrix metalloproteinase-7 disrupts dendritic spines in hippocampal neurons through NMDA receptor activation. *J. Neurochem.* **97**, 44–56.

Bixby J. L., Grunwald G. B. and Bookman R. J. (1994) Ca^{2+} influx and neurite growth in response to purified N-cadherin and laminin. *J. Cell Biol.* **127**, 1461–1475.

Bowers M. S., McFarland K., Lake R. W., Peterson Y. K., Lapish C. C., Gregory M. L., Lanier S. M. and Kalivas P. W. (2004) Activator of G protein signaling 3: a gatekeeper of cocaine sensitization and drug seeking. *Neuron* **42**, 269–281.

Bowyer J. F. and Weiner N. (1987) Modulation of the Ca^{2+}-evoked release of [3H]-dopamine from striatal synaptosomes by dopamine (D2) agonists and antagonists. *J. Pharmacol. Exp. Ther.* **241**, 27–33.

Frankin K. B. J. and Paxinos G. (1997) *The mouse brain in stereotaxic coordinates*. Academic, San Diego.

Freyer A. M., Bilington C. K., Penn R. B. and Hall I. P. (2004) Extracellular matrix modulates β2-adrenergic receptor signaling in human airway smooth muscle cells. *Am. J. Respir. Cell Mol. Biol.* **31**, 440–445.

Goldstein R. Z. and Volkow N. D. (2002) Drug addiction and its underlying neurobiological basis: neuroimaging evidence for the involvement of the frontal cortex. *Am. J. Psychiatry* **159**, 1642–1652.

Hashimoto T., Matsumoto M. M., Li J. F., Lawton M. T. and Young W. L. (2005) Suppression of MMP-9 by doxycycline in brain arteriovenous malformations. *BMC Neurology* **5**, 1.

Itoh T., Ikeda T., Gomi H., Nakao S., Suzuki T. and Itohara S. (1997) Unaltered secretion of β-amyloid precursor protein in gelatinase A (matrix metalloproteinases 2)-deficient mice. *J. Biol Chem.* **272**, 22389–22392.

Kaczmarek L., Lapinska-Dzwonek J. and Szymczak S. (2002) Matrix metalloproteinases in the adult brain physiology: a link between c-Fos, AP-1 and remodeling of neuronal connections? *EMBO J.* **21**, 6643–6648.

Kattenstroth G., Tantalaki E., Sudhof T. C., Gottmann K. and Missler M. (2004) Postsynaptic *N*-methyl-D-aspartate receptor function requires α-neurexins. *Proc. Natl Acad. Sci. USA* **101**, 2607–2612.

Khokha R., Waterhouse P., Yagel S., Lala P. K., Overall C. M., Norton G. and Denhardt D. T. (1989) Antisense RNA-induced reduction in murine TIMP levels confers oncogenicity on Swiss 3T3 cells. *Science* **243**, 947–950.

Koivunen E., Arap W., Valtanen H. *et al.* (1999) Tumor targeting with a selective gelatinase inhibitor. *Nat. Biotechnol.* **17**, 768–774.

Lee S. R., Tsuji K., Lee S. R. and Lo E. H. (2004) Role of matrix metalloproteinases in delayed neuronal damage after transient global cerebral ischemia. *J. Neurosci.* **24**, 671–678.

Lindgren N., Xu Z-Q., Herrera-M M., Haycock J., Hokfelt T. and Fisone G. (2001) Dopamine D2 receptors regulate tyrosine hydroxylase activity and phosphorylation at Ser40 in rat striatum. *Eur. J. Neurosci.* **13**, 773–780.

Mannello F. and Gazzanelli G. (2001) Tissue inhibitors of metalloproteinases and programmed cell death: conundrums, controversies and potential implications. *Apoptosis* **6**, 479–482.

Mizoguchi H., Yamada K., Mizuno M., Mizuno T., Nitta A., Noda Y. and Nabeshima T. (2004) Regulations of methamphetamine reward by extracellular signal-regulated kinase 1/2/ets-like gene-1 signaling pathway via the activation of dopamine receptors. *Mol. Pharmacol.* **65**, 1293–1301.

Mizoguchi H., Yamada K., Niwa M., Mouri A., Mizuno T., Noda Y., Nitta A., Itohara S., Banno Y. and Nabeshima T. (2007) Reduction of methamphetamine-induced sensitization and reward in matrix metalloproteinase-2 and -9 deficient mice. *J. Neurochem.* **100**, 1579–1588.

Nagai T., Yamada K., Yoshimura M., Ishikawa K., Miyamoto Y., Hashimoto K., Noda Y., Nitta A. and Nabeshima T. (2004) The tissue plasminnogen activator-plasmin system participates in the rewarding effect of morphine by regulating dopamine release. *Proc. Natl Acad. Sci. USA* **101**, 3650–3655.

Nagai T., Noda Y., Ishikawa K., Miyamoto Y., Yoshimura M., Ito M., Takayanagi M., Takuma K., Yamada K. and Nabeshima T. (2005) The role of tissue plasminogen activator in methamphetamine-related reward and sensitization. *J. Neurochem.* **92**, 660–667.

Nagy V., Bozdagi O., Matynia A., Balcerzyk M., Okulski P., Dzwonek J., Costa R. M., Silva A. J., Kaczmarek L. and Huntley G. W. (2006) Matrix metalloproteinase-9 is required for hippocampal late-phase long-term potentiation and memory. *J. Neurosci.* **15**, 1923–1934.

Nakagawa T., Kubota T., Kabut M., Sato K., Kawano H., Hayakawa T. and Okada Y. (1994) Production of matrix metalloproteinases and tissue inhibitor of metalloproteinases-1 by human brain tumors. *J. Neurosurg.* **81**, 69–77.

Nakajima A., Yamada K., Nagai T. *et al.* (2004) Role of tumor necrosis factor-alpha in methamphetamine-induced drug dependence and neurotoxicity. *J. Neurosci.* **24**, 2212–2225.

Nestler E. J. (2001) Molecular basis of long-term plasticity underlying addiction. *Nat. Rev. Neurosci.* **2**, 119–128.

Paxinos G. and Watson C. (1982) *The Rat Brain in Stereotaxic Coordinates*. Academic, New York.

Reeves T., Prins M. L., Zhu J. P., Povlishock J. T. and Phillips L. L. (2003) Matrix metalloproteinases inhibition alters functional and structural correlates of deafferentation-induced sprouting in the dentate gyrus. *J. Neurosci.* **12**, 10182–10189.

Rivera S., Tremblay E., Timsit S., Canals O., Ben-Ari Y. and Khrestchatisky M. (1997) Tissue inhibitor of metalloproteinases-1 (TIMP-1) is differentially induced in neurons and astrocytes after seizures: evidence for developmental, immediate early gene, and lesion response. *J. Neurosci.* **17**, 4223–4235.

Robinson T. E. and Kolb B. (1997) Persistent structural modifications in nucleus accumbens and prefrontal cortex neurons produced by previous experience with amphetamine. *J. Neurosci.* **17**, 8491–8497.

Rosenberg G. A., Kornfeld M., Estrada E., Kelly R. O., Liotta L. A. and Stetler-Stevenson W. G. (1992) TIMP-2 reduces proteolytic opening of blood-brain barrier by IV collagenagse. *Brain Res.* **56**, 203–207.

Shippenberg T. S. and Heidbreder C. h. (1995) Sensitization to the conditioned rewarding effects of cocaine: pharmacological and temporal characteristics. *J. Pharmacol. Exp. Ther.* **273**, 808–815.

Smith G. N. J., Brandt K. D. and Hasty K. A. (1996) Activation of recombinant human neutrophil procollagenase in the presence of doxycycline results in fragmentation of the enzyme and loss of enzyme activity. *Arthritis Rheum.* **39**, 235–244.

Sternlicht M. D. and Werb Z. (2001) How matrix metalloproteinases regulate cell behavior. *Annu. Rev. Cell Dev. Biol.* **17**, 463–516.

Strongin A. Y., Collier I., Bannikov G., Marmer B. L., Grant G. A. and Goldberg G. I. (1995) Mechanism of cell surgace activation of 72-kDa type IV collagenase Isolation of the activated form of the membrane metalloproteinases. *J. Biol. Chem.* **270**, 5331–5338.

Sülzer D., Chen T. K., Lau Y. Y., Kristensen H., Rayport S. and Ewing A. (1995) Amphetamine redistributes dopamine from synaptic vesicles to the cytosol and promotes reverse transport. *J. Neurosci.* **15**, 4102–4108.

Sunderland W. J., Son Y. J., Miner J. H., Sanes J. R. and Carlson S. S. (2000) The presynaptic calcium channel is part of a transmembrane complex linking a synaptic laminin ($\alpha4\beta2\gamma1$) with non-erythroid spectrin. *J. Neurosci.* **20**, 1009–1019.

Szklarczyk A., Lapinska J., Rylski M., Mckay R. D. and Kaczmarek L. (2002) Matrixmetalloproteinase-9 undergoes expression and activation during dendritic remodeling in adult hippocampus. *J. Neurosci.* **22**, 920–930.

Uitto V. J., Firth J., Nip L. and Golub L. (1994) Doxycycline and chemically modified tetracyclines inhibit gelatinase A (MMP-2) gene expression in human skin keratinocytes. *Ann. NY Acad. Sci.* **732**, 140–151.

Ushkaryov Y. A., Petrenko A. G., Geppert M. and Sudhof T. C. (2002) Neurexins: synaptic cell surface proteins related to the alpha-latrotoxin receptor and laminin. *Science* **257**, 50–56.

Vaillant C., Didier-Bazes M., Hurter A., Bein M. F. and Thomasset N. (1999) Spatiotemporal expression patterns of metalloproteinases and their inhibitors in the postnatal developing rat cerebellum. *J. Neurosci.* **19**, 4994–5004.

Wright J. W., Reichert J. R., Davis C. J. and Harding J. W. (2002) Neural plasticity and the brain renin-angiotensin system. *Neurosci. Biobehav. Rev.* **26**, 529–552.

Yamada K., Nagai T. and Nabeshima T. (2005) Drug dependence, synaptic plasticity, and tissue plasminogen activator. *J. Pharmacol. Sci.* **97**, 157–161.

Yong V. W., Power C., Forsyth P. and Edwards D. R. (2001) Metalloproteinases in biology and pathology of the nervous system. *Nat. Rev. Neurosci.* **2**, 502–511.

Zhang J. W. and Gottschall P. E. (1997) Zymographic measurement of gelatinase activiy in brain tissue after detergent extrqaction and affinity-support purification. *J. Neurosci. Methods* **76**, 15–20.

Behavioral/Systems/Cognitive

A Novel Molecule "Shati" Is Involved in Methamphetamine-Induced Hyperlocomotion, Sensitization, and Conditioned Place Preference

Minae Niwa,[1,3] Atsumi Nitta,[1] Hiroyuki Mizoguchi,[1] Yasutomo Ito,[2] Yukihiro Noda,[1] Taku Nagai,[1] and Toshitaka Nabeshima[1,3]

[1]Department of Neuropsychopharmacology and Hospital Pharmacy and [2]Equipment Center for Research and Education, Nagoya University Graduate School of Medicine, Nagoya 466-8560, Japan, and [3]Department of Chemical Pharmacology, Meijo University Graduate School of Pharmaceutical Sciences, Nagoya 468-8503, Japan

Drug addiction places an enormous burden on society through its repercussions on crime rate and healthcare. Repeated exposure to drugs of abuse causes cellular adaptations in specific neuronal populations that ultimately can lead to a state of addiction. In the present study, we have identified a novel molecule "shati" from the nucleus accumbens (NAc) of mice treated with methamphetamine (METH) using the PCR-select complementary DNA subtraction method. Moreover, we investigated whether shati is involved in METH-induced hyperlocomotion, sensitization, and conditioned place preference (CPP). METH induced expression of shati mRNA dose dependently via dopamine (DA) receptors. We prepared antibodies against shati and, using them, found shati to be expressed in neuronal cells of the mouse brain. Treatment with the shati antisense oligonucleotide (shati-AS), which significantly inhibited the expression of shati mRNA, enhanced the acute METH response, METH-induced behavioral sensitization, and CPP. Blockage of shati mRNA by shati-AS potentiated the METH-induced increase of DA overflow in the NAc and the METH-induced decrease in synaptosomal and vesicular DA uptake in the midbrain. These results suggest that a novel molecule shati is involved in the development of METH-induced hyperlocomotion, sensitization, and CPP. The functional roles of shati in METH-regulated behavioral alternations are likely to be mediated by its inhibitory effects on the METH-induced increase of DA overflow in the NAc and the METH-induced decrease in DA uptake in the midbrain.

Key words: **shati; methamphetamine; behavioral sensitization; conditioned place preference; dopamine; addiction**

Introduction

In terms of lost lives and productivity, drug dependence remains one of the most serious threats to the public health of a nation (Nestler, 2002). Drugs of abuse, including methamphetamine (METH), modulate the activity of mesolimbic dopaminergic neurons, projecting from the ventral tegmental area (VTA) to the nucleus accumbens (NAc) (Koob, 1992; Wise, 1996b; Koob et al., 1998). The psychostimulatory effects of METH are associated with an increase in extracellular dopamine (DA) levels in the brain, by facilitating the release of DA from presynaptic nerve terminals and inhibiting reuptake (Heikkila et al., 1975; Seiden et al., 1993; Giros et al., 1996). In rodent, augmentation of behavioral responses to psychostimulants is observed during and after their repeated administration. Therefore, it has been proposed that activity-dependent synaptic plasticity and remodeling of the mesolimbic dopaminergic system may play a crucial role in drug dependence (Nestler, 2001; Yamada and Nabeshima, 2004).

Using cDNA microarrays, changes in the mRNA expression profile in relevant brain regions (e.g., NAc) have been assessed after chronic administration of abused drugs (Douglass and Daoud, 1996; Cha et al., 1997; Wang et al., 1997). Evidence from this line of research has implicated nuclear factor-κB (Ang et al., 2001) and ΔFosB (Zachariou et al., 2006) in signal transduction pathways that modulate behavioral effects induced by drugs and contribute to long-term neuronal changes associated with dependence (Laakso et al., 2002). To elucidate the mechanism, caused by chronic drug abuse, of stable changes in the brain that play a role in the long-lasting behavioral abnormalities of dependent subjects, the candidates for drug-dependence-related genes

Received Dec. 18, 2006; revised May 21, 2007; accepted May 21, 2007.

This work was supported in part by a Grant-in-Aid for Scientific Research and Special Coordination Funds for Promoting Science and Technology, Target-Oriented Brain Science Research Program; a Grant-in-Aid for Scientific Research (B), Exploratory Research, and Young Scientists (A); the 21st Century Center of Excellence Program "Integrated Molecular Medicine for Neuronal and Neoplastic Disorders" from the Ministry of Education, Culture, Sports, Science, and Technology of Japan; a Grant-in-Aid for Health Science Research on Regulatory Science of Pharmaceuticals and Medical Devices, and Comprehensive Research on Aging and Health from the Ministry of Health, Labor, and Welfare of Japan; a Smoking Research Foundation Grant for Biomedical Research; a grant from the Brain Research Center from the 21st Century Frontier Research Program funded by the Ministry of Science and Technology, Republic of Korea; by the Japan Canada Joint Health Research Program; and by a grant from Takeda Science Foundation. We are grateful to Drs. Kenji Kadomatsu, Yoshifumi Takei, and Hanayo Kawai (Department of Biochemistry, Nagoya University Graduate School of Medicine, Nagoya, Japan) for technical assistance, critical comments, and helpful discussions. We also thank Dr. Noboru Ogiso, Yasutaka Ohya, Yuuki Ushiro, and Kazumi Kawai (Division for Research of Laboratory Animals, Center for Research of Laboratory Animals and Medical Research Engineering, Nagoya University Graduate School of Medicine) and Nobuyoshi Hamada and Yoshiyuki Nakamura (Radioisotope Center Medical Branch, Nagoya University Graduate School of Medicine) for technical assistance.

Correspondence should be addressed to Dr. Toshitaka Nabeshima, Department of Chemical Pharmacology, Meijo University Graduate School of Pharmaceutical Sciences, 150 Yagotoyama, Tenpaku-ku, Nagoya 468-8503, Japan. E-mail: tnabeshi@ccmfs.meijo-u.ac.jp.

DOI:10.1523/JNEUROSCI.1575-07.2007

 0270-6474/07/277604-12$15.00/0

whose expression was altered by repeated administration of METH or morphine (MOR) were screened by using cDNA microarray. Recently, there are many studies that showed that cytokines/neurotrophic factors and extracellular matrix/proteases play critical roles in activity-dependent synaptic plasticity and remodeling of the mesocorticolimbic dopaminergic system (Horger et al., 1999; Messer et al., 2000; Mizoguchi et al., 2007). We found that tumor necrosis factor-α (TNF-α) plays a neuroprotective role in METH-induced dependence and neurotoxicity (Nakajima et al., 2004) and reduces MOR-induced rewarding effects and behavioral sensitization (Niwa et al., 2007a,d). Furthermore, the rewarding effects and sensitization induced by METH and MOR are attenuated by Leu-Ile, an inducer of TNF-α, and glial cell line-derived neurotrophic factor (GDNF) (Niwa et al., 2007a–d). The tissue plasminogen activator (tPA)–plasmin system potentiates the rewarding and locomotor-stimulating effects of METH, MOR, and nicotine by regulating release of DA (Nagai et al., 2004, 2005a,b, 2006). However, the exact neuronal circuits and molecular cascade essential for drug dependence remain unclear. Therefore, we attempt to explore the novel molecules that play more critical roles in drug dependence, because the functions of molecules targeted by DNA microarray screening have been already well known.

In the present study, we identified a novel molecule "shati" from the NAc of mice treated with METH using the PCR-select cDNA subtraction method, which is a differential and epochal cloning technique. Moreover, we demonstrated that shati is involved in the METH-induced hyperlocomotion, sensitization, and conditioned place preference (CPP).

Materials and Methods

Animals. The male C57BL/6J inbred mice were obtained from SLC Japan (Hamamatsu, Japan). Animals were housed in plastic cages and kept in a temperature-, humidity-, and light-controlled room (23 ± 1°C; 50 ± 5% humidity; 12 h light/dark cycle starting at 8:00 A.M.) and had *ad libitum* access to food and water, except during behavioral experiments. All animal care and use was in accordance with the National Institutes of Health *Guide for the Care and Use of Laboratory Animals* and approved by the Institutional Animal Care and Use Committee of Nagoya University School of Medicine. Animals were treated according to the *Guidelines of Experimental Animal Care* issued from the Office of the Prime Minister of Japan.

PCR-select cDNA subtraction. Mice were administered METH (2 mg/kg, s.c.) or saline for 6 d and took NAc 2 h after the last injection of METH. PCR-select cDNA subtraction (Clontech, Palo Alto, CA) was performed using a previously established procedure (Diatchenko et al., 1996; Gurskaya et al., 1996) to detect the genes in the NAc affected by METH treatment. Briefly, they involve hybridization of cDNA from one population (tester; METH-treated NAc) to excess of mRNA (cDNA) from other population (driver; saline-treated NAc) and then separation of the unhybridized fraction (target) from hybridized common sequences. Total RNAs were extracted by RNeasy Max (Qiagen, Hilden, Germany). For each subtraction, we performed two PCR amplifications. Products from the secondary PCRs were inserted into pCRII using a T/A cloning kit (Invitrogen, Carlsbad, CA). Plasmid or cosmid DNAs were prepared using QIAwell 8 Plus kit (Qiagen) according to the protocol of the manufacturer. Nucleic acid homology searches were performed using the BLAST (basic local alignment search tool) program through e-mail servers at the National Center for Biotechnology Information (NCBI) (National Institutes of Health, Bethesda, MD).

Structure models. Homology modeling for C-terminal domain of shati was established using Molecular Operating Environment (MOE) software (Chemical Computing Group, Montreal, Quebec, Canada). Molecular mechanics calculations were performed by using an MMFF94x force field. Docking simulations of acetyl-CoA or ATP with shati protein were also examined using MOE software (Chemical Computing Group) to calculate the interactive potential energy of molecules.

Table 1. Primers sequences and their targets for RT-PCR

Primer	Sequence	Target (bp)
1		
Forward	5′-CTTGCCTCCCCAGCCCATCA-3′	1987–2006
Reverse	5′-CTGGGGGCCAGGGTTCTGCT-3′	2147–2166
2		
Forward	5′-GGGTGGCCGGGTAGGTGGAA-3′	2909–2928
Reverse	5′-GGCAGTGCCCAGCCCTTCCT-3′	3073–3092
3		
Forward	5′-TGTACATTCCTCCCTGGTGGTG-3′	3521–3542
Reverse	5′-AAATCTGAGAGCTGCAAGAAAATAGGG-3′	3594–3620

The amplification consisted of an initial step (95°C for 5 min) and then 35 cycles of denaturation for 30 s at 94°C and annealing for 1 min at 70, 71, and 65°C.

Reverse transcription-PCR and real-time reverse transcription-PCR. Mice were administered METH (0.3, 1, and 2 mg/kg, s.c., once a day for 3 or 6 d) and decapitated 2 h after the last injection of METH. In the real-time reverse transcription (RT)-PCR experiment on the antagonism of METH-induced shati mRNA expression, mice were treated with the DA D_1-like receptor antagonist *R*(+)-SCH23390 [*R*(+)-7-chloro-8-hydroxy-3-methyl-1-phenyl-2,3,4,5-tetrahydro-1*H*-3-benzazepine] (0.1 mg/kg, i.p.) or DA D_2-like receptor antagonist raclopride (2 mg/kg, i.p.) 30 min before METH (2 mg/kg, s.c.) once a day for 6 d. Functionally, *R*(+)-SCH23390 (0.1–0.5 mg/kg) is a potent blocker of stereotyped behaviors and increased locomotion induced by amphetamine or apomorphine (Christensen et al., 1984; Napier et al., 1986). The increase in TNF-α or tPA mRNA expression in the NAc induced by METH is inhibited by pretreatment with either *R*(+)-SCH23390 (0.1 or 0.5 mg/kg, i.p.) or raclopride (2 mg/kg, i.p.) (Nakajima et al., 2004; Nagai et al., 2005a). *R*(+)-SCH23390 at the dose of 0.1 mg/kg, not 0.03 mg/kg, significantly inhibits the hyperphosphorylation of extracellular signal-regulated kinase 1/2 in the NAc and striatum evoked by METH-induced CPP as well as the expression of CPP in METH-treated animals (Mizoguchi et al., 2004). Depending on these evidences, we selected the doses of *R*(+)-SCH23390 at 0.1 mg/kg and raclopride at 2 mg/kg.

Total RNA was isolated using an RNeasy kit (Qiagen) and converted into cDNA using a SuperScript First-Strand System for RT-PCR kit (Invitrogen). The primers used for RT-PCR were as follows: 5′-CTTGCCTCCCCAGCCCATCA-3′ (forward-1; base pairs 1987–2006) and 5′-CTGGGGGCCAGGGTTCTGCT-3′ (reverse-1; base pairs 2147–2166) for set of sequences 1; 5′-GGGTGGCCGGGTAGGTGGAA-3′ (forward-2; base pairs 2909–2928) and 5′-GGCAGTGCCCAGCCCTTCCT-3′ (reverse-2; base pairs 3073–3092) for set of sequences 2; and 5′-TGTACATTCCTCCCTGGTGGTG-3′ (forward-3; base pairs 3521–3542) and 5′-AAATCTGAGAGCTGCAAGAAAATAGGG-3′ (reverse-3; base pairs 3594–3620) for set of sequences 3 (Table 1). The amplification consisted of an initial step (95°C for 5 min) and then 35 cycles of denaturation for 30 s at 94°C and annealing for 1 min at 70, 71, and 65°C in a GeneAmp PCR System 9700 (Applied Biosystems, Foster City, CA). The levels of shati and TNF-α mRNA were determined by real-time RT-PCR using a TaqMan probe. The 18S ribosomal RNA was used as the internal control (PE Applied Biosystems, Foster City, CA). The mouse shati primers used for real-time RT-PCR were as follows: 5′-TGTAAACACCCCTAAAGTGCCCT-3′ (forward; base pairs 2967–2989) and 5′-TCAATCCTGCATACAAGGAATCAA-3′ (reverse; bare pairs 3022–3045); and TaqMan probe, 5′-CACAGTCTGTGAGGCTCAGGTTGCCC-3′ (probe; base pairs 2995–3020). The amplification consisted of an initial step (95°C for 5 min) and then 40 cycles of denaturation for 30 s at 95°C and annealing for 1 min at 59°C in an iCycle iQ Detection System (Bio-Rad, Hercules, CA). The expression levels were calculated as described previously (Wada et al., 2000).

Immunohistochemistry. Two antibodies against the peptide of the hypothetical protein, CNTAFRGLRQHPRTQLL (S-3) and CMSVDSRFRGKGIAKALG (S-4), unique to shati were generated. These peptides were conjugated to the keyhole limpet hemocyanin and injected into rabbits six times at 1 week intervals. Serum was taken from the rabbits 1

week after the final injection of these peptides. The serum was diluted 200 times used for the immunostaining.

For immunohistochemical analysis, mice were killed 24 h after repeated treatment with METH (2 mg/kg, s.c., once a day for 6 d). The brains were sliced at 20 μm in the cryostat. Polyclonal rabbit anti-S-3 or S-4 antibody (1:200), monoclonal mouse anti-neuron-specific nuclear antigen (NeuN) antibody (1:200; Chemicon, Temecula, CA), and monoclonal mouse anti-glial fibrillary acidic protein (GFAP) antibody (1:200; Chemicon) served as primary antibodies. Goat anti-mouse Alexa Fluor 546 (1:1000; Invitrogen) and goat anti-rabbit Alexa Fluor 488 (1:1000; Invitrogen) were used as secondary antibodies. Each stained slice was observed under a fluorescence microscope (Axioskoop 2 plus; Zeiss, Jena, Germany) and checked with Axiovision 3.0 systems (Zeiss).

Shati-antisense oligonucleotide treatment. Mice were anesthetized with pentobarbital (40 mg/kg, i.p.) and placed in a stereotaxic apparatus. The infusion cannula was connected to a miniosmotic pump (total capacity was 90 μl, Alzet 1002; Alza, Palo Alto, CA) filled with shati-antisense oligonucleotide (shati-AS) and -scramble oligonucleotide (shati-SC) and was implanted into the right ventricle [anteroposterior (AP) −0.5 mm, mediolateral (ML) +1.0 mm from the bregma, and dorsoventral (DV) −2.0 mm from the skull, according to the atlas of Franklin and Paxinos (1997)]. No histological or mechanical disruption was produced by implantation of the infusion cannula (data not shown). Phosphorothionate oligonucleotides were custom synthesized at Nisshinbo Biotechnology (Tokyo, Japan) and dissolved in artificial CSF (in mM: 147 NaCl, 3 KCl, 1.2 $CaCl_2$, and1.0 $MgCl_2$, pH 7.2). We used shati-SC as a control of shati-AS, because we should deny the secondary effects on other genes or toxic effects, and we selected the design of shati-AS, which does not affect the other genes and already have been identified. The oligonucleotides were phosphorothionated at the three bases of both 5′ and 3′ ends, which results in increased stability and less toxicity. The sequences of shati-AS and shati-SC were 5′-TCTTCGTCTCGCAGACCATGTCG-3′ and 5′-GGTCTGCTACACTGCTGCTAGTC-3′, respectively. Shati-AS and shati-SC were continuously infused into the cerebral ventricle at a dose of 1.8 nmol/6 μl per day (flow rate, 0.25 μl/h). Additionally, shati-SC was used as a control. Three days after the start of oligonucleotide infusion, mice were subjected to METH treatment for sensitization.

Locomotor activity. Locomotor activity was measured using an infrared detector (Neuroscience Company, Tokyo, Japan) in a plastic box (32 × 22 × 15 cm high) and determined as described previously (Nakajima et al., 2004; Niwa et al., 2007b,d). One day after the start of oligonucleotide infusion, mice were habituated for 3 h in the box for 2 d and then administered METH (1 mg/kg, s.c.) or saline once a day for 5 d. Locomotor activity was measured for 2 h immediately after the METH or saline administration.

In vivo *microdialysis.* Mice were anesthetized with sodium pentobarbital, and a guide cannula (AG-8; EICOM, Kyoto, Japan) was implanted into the NAc (AP +1.7 mm, ML +0.8 mm mediolateral from the bregma, and DV −4.0 mm from the skull) according to the atlas of Franklin and Paxinos (1997) and secured to the skull using stainless steel screws and dental acrylic cement. Mice were administered METH (1 mg/kg, s.c.) 3 d after implantation of the guide cannula and the start of oligonucleotide infusion. One day after METH treatment for 2 d, a dialysis probe (AI-8-1, 1 mm membrane length; EICOM) was inserted through the guide cannula and perfused continuously with CSF (in mM: 147 NaCl, 4 KCl, and 2.3 $CaCl_2$) at a flow rate of 1.0 μl/min. Dialysate was collected in 20 min fractions and injected into the HPLC system (EICOM) for the measurement of DA levels. Three samples were used to establish baseline levels of DA before the administration of METH (1 mg/kg, s.c.).

Synaptosomal [^{3}H]DA uptake. Three days after the start of oligonucleotide infusion, mice were subjected to METH treatment once a day for 3 d. Mice were decapitated 1 h after the final METH treatment. Midbrain synaptosomal [^{3}H]DA uptake was determined as described previously (Fleckenstein et al., 1997; Nakajima et al., 2004; Niwa et al., 2007b). The final concentration of [^{3}H]DA (PerkinElmer, Wellesley, MA) was 5 nM. Samples were incubated at 37°C for 4 min, and then ice-cold Krebs–Ringer's solution containing 10 μM GBR12909 [1-(2[bis(4-fluorophenyl-)methoxy]ethyl)-4-(3-phenylpropyl)piperazine] bimesylate hydrate] (Sigma, St. Louis, MO), a specific DA uptake inhibitor, was added. Nonspecific values were determined in the presence of 100 μM GBR12909 during the incubation. The radioactivity trapped on filters was measured with a liquid scintillation counter (Beckman Coulter, Fullerton, CA).

Vesicular [^{3}H]DA uptake. Vesicular [^{3}H]DA uptake was determined as described by Erickson et al. (1990). Synaptosomes were prepared as described by Nakajima et al. (2004). Vesicular [^{3}H]DA uptake was performed by incubating synaptic vesicle samples (15 μg protein/100 μl) at 30°C for 4 min in assay buffer (in mM: 25 HEPES, 100 potassium tartrate, 1.7 ascorbic acid, 0.05 EGTA, 0.1 EDTA, and 2 ATP-Mg^{2+}, pH 7.0) in the presence of 30 nM [^{3}H]DA (PerkinElmer). The reaction was terminated by the addition of 1 ml of cold wash buffer (assay buffer containing 2 mM $MgSO_4$ substituted for the ATP-Mg^{2+}, pH 7.0) and rapid filtration. Nonspecific values were determined by measuring vesicular [^{3}H]DA uptake at 4°C. The radioactivity was measured with a liquid scintillation counter (Beckman Coulter).

Conditioned place preference. The apparatus used for the place conditioning task consisted of two compartments: a transparent Plexiglas box and a black Plexiglas box (both 15 × 15 × 15 cm high). To enable mice to distinguish easily the two compartments, the floors of the transparent and black boxes were covered with white plastic mesh and black frosting Plexiglas, respectively. Each box could be divided by a sliding door (10 × 15 cm high). The place conditioning paradigm was performed by using a previously established procedure with a minor modification (Noda et al., 1998; Schechter and Calcagnetti, 1998; Niwa et al., 2007a,b,d). In the preconditioning test, the sliding door was opened, and the mouse was allowed to move freely between both boxes for 15 min once a day for 3 d. On the third day of the preconditioning test, we measured the time that the mouse spent in the black and transparent boxes by using a Scanet SV-20 LD (Melquest, Toyama, Japan). The box in which the mouse spent the most time was referred to as the "preferred side" and the other box as the "nonpreferred side." Conditioning was performed during 6 successive days. Mice were given METH or saline in the apparatus with the sliding door closed. That is, a mouse was subcutaneously given METH and put in its nonpreferred side for 20 min. On the next day, the mouse was given saline and placed opposite the drug conditioning site for 20 min. These treatments were repeated for three cycles (6 d). In the postconditioning test, the sliding door was opened, and we measured the time that the mouse spent in the black and transparent boxes for 15 min, using the Scanet SV-20 LD. Place conditioning behavior was expressed by Post-Pre, which was calculated as: [(postvalue) − (prevalue)], where postvalue and prevalue were the difference in time spent at the drug conditioning and the saline conditioning sites in the postconditioning and preconditioning tests, respectively.

Statistical analysis. All data were expressed as means ± SE. Statistical differences between two groups were determined with Student's *t* test. Statistical differences among more than three groups were determined using a one-way ANOVA, two-way ANOVA, or an ANOVA with repeated measures (two or three-factor), followed by the Bonferroni's multiple comparison test (Bonferroni's correction; 3, 6, 15, and 36 comparisons in 3, 4, 6, and 9 groups, respectively). $p < 0.05$ was regarded as statistically significant.

Nucleotide sequences. The DNA Data Bank of Japan/GenBank/European Molecular Biology Laboratory accession number for the primary nucleotide sequence of shati is DQ174094.

Results

Identification of shati

The reasons why we pursued shati for intensive investigation arose from our preliminary findings with the PCR-select cDNA subtraction method to detect the genes in the NAc affected by METH treatment: mice were administrated METH (2 mg/kg, s.c.) or saline for 6 d, and shati mRNA production in the NAc was found to increase by 640% in METH-treated mice with robust behavioral sensitization compared with saline-treated mice (data not shown). The sequence of cDNA was completely matched to accession number NM_001001985 of NCBI gene bank (the gene

record was replaced by accession number NM_001001985.2 on April, 10, 2005). The sequence has been identified by the Mammalian Gene Collection Program Team (Strausberg et al., 2002). Blackshaw et al. (2004) has demonstrated the extended cDNA sequence by serial analysis of gene expression methods, which provides an unbiased and nearly comprehensive readout of gene expression and that the gene was for one of the proteins related to the retina development. We named this novel molecule shati after the symbol at Nagoya castle in Japan. The sequence is translated to a protein LOC269642 (accession number is NP_001001985.1 and 2; 001001985.1 was a part of 001001985.2) (supplemental Fig. 1, available at www.jneurosci.org as supplemental material).

Characterization of shati

Homology modeling for C-terminal domain of shati was established using MOE software (Chemical Computing Group) (Fig. 1*A*,*B*). Red character in Figure 1*A* showed homology modeling of shati. From motif analysis of shati, shati contained the sequence of GCN5-related *N*-acetyltransferase (GCAT) (Fig. 1*C*). Underlined character in Figure 1*A* showed GNAT motif. Docking simulations of acetyl-CoA or ATP with shati protein were also examined using MOE software (Chemical Computing Group) to calculate the interactive potential energy of molecules. Shati also contained acetyl-CoA binding or ATP binding site, because the analysis showed the lowest interactive potential energy of shati with acetyl-CoA or ATP, −301 and −322 kcal, respectively (supplemental Fig. 2, available at www.jneurosci.org as supplemental material). Docking simulations of shati with DA, DNA binding site, and nuclear localization signals showed too high interactive potential energy of molecules or no domain.

Expression of shati mRNA

As shown in Figure 2*A*, RT-PCR analysis revealed that shati is expressed at high levels in the cerebrum, cerebellum, liver, kidney, and spleen. We amplified and analyzed its three different target sequences by RT-PCR (Table 1). Similar results of RT-PCR were obtained with three different sets of primers (Fig. 2*A*).

We performed a series of experiments to validate the results of cDNA subtraction. Repeated METH treatment (2 mg/kg, s.c.) for 6 d significantly elevated the mRNA levels of the target sequences of shati in the NAc (Fig. 2*B*).

METH-induced expression of shati mRNA in the brain

As an initial step in assessing the relationship between shati and METH-induced sensitization and dependence, we examined whether single and repeated METH treatment altered the expression of shati mRNA in the mouse brain using the real-time RT-PCR method. The effects of repeated METH treatment (0.3, 1 and 2 mg/kg, s.c. for 3 d) on shati mRNA expression in the NAc were dose dependent ($F_{(3,28)} = 5.503$; $p < 0.01$, one-way ANOVA) (Fig. 3*A*). The levels of shati mRNA were significantly increased 2, 6, and 24 h after the last METH treatment and then returned to control value 1 week after the treatment ($F_{(6,41)} = 4.444$; $p < 0.01$, one-way ANOVA) (Fig. 3*B*). Single METH treatment (2 mg/kg, s.c.) remarkably induced shati mRNA expression in the NAc and hippocampus (Hip). METH (2 mg/kg, s.c.) or saline challenge on day 6 after repeated administration of METH (2 mg/kg, s.c.) for 5 d remarkably induced shati mRNA expression in the frontal cortex (Fc), NAc, and caudate–putamen (CPu) (repeated drug administration, $F_{(1,32)} = 20.368$, $p < 0.01$ for Fc; single administration, $F_{(1,32)} = 0.005$, $p = 0.942$ for Fc; repeated drug administration × single administration, $F_{(1,32)} = 1.643$, $p = 0.209$ for Fc; repeated drug administration, $F_{(1,31)} = 14.436$, $p <$

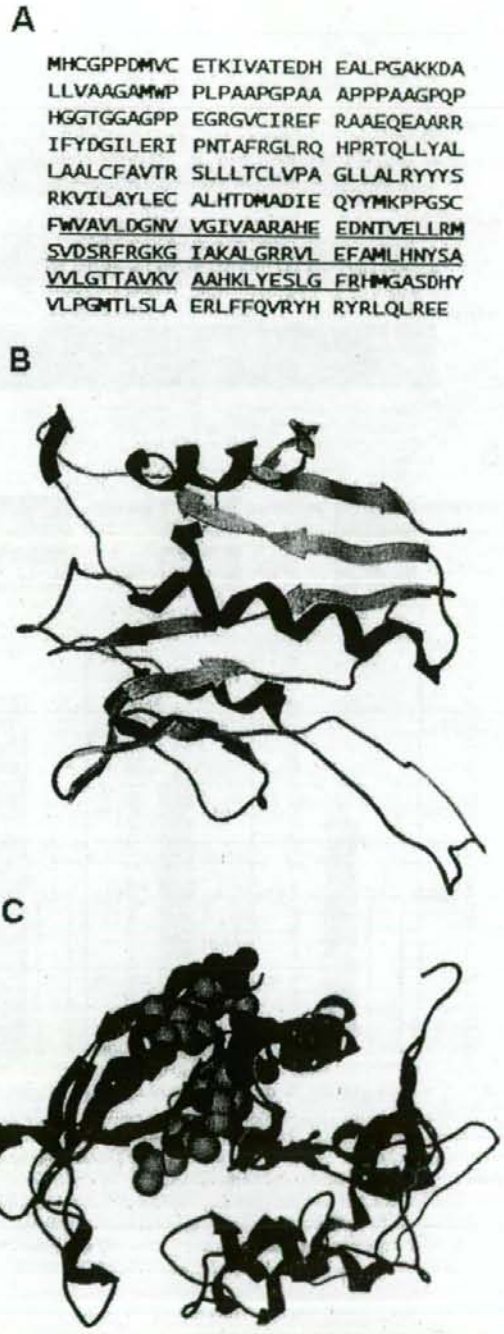

Figure 1. Characterization of shati. *A*, The sequence of shati. The red character showed homology modeling of shati. The underlined character showed GCN5-related *N*-acetyltransferase motif. *B*, Homology modeling for C-terminal domain of shati. *C*, Homology modeling and motif analysis of shati. Shati has the sequence of GCAT. Red ribbon, Homology model of shati; sphere, acetyl-CoA analyzed by x-ray crystallography; green ribbon, *N*-acetyltransferase.

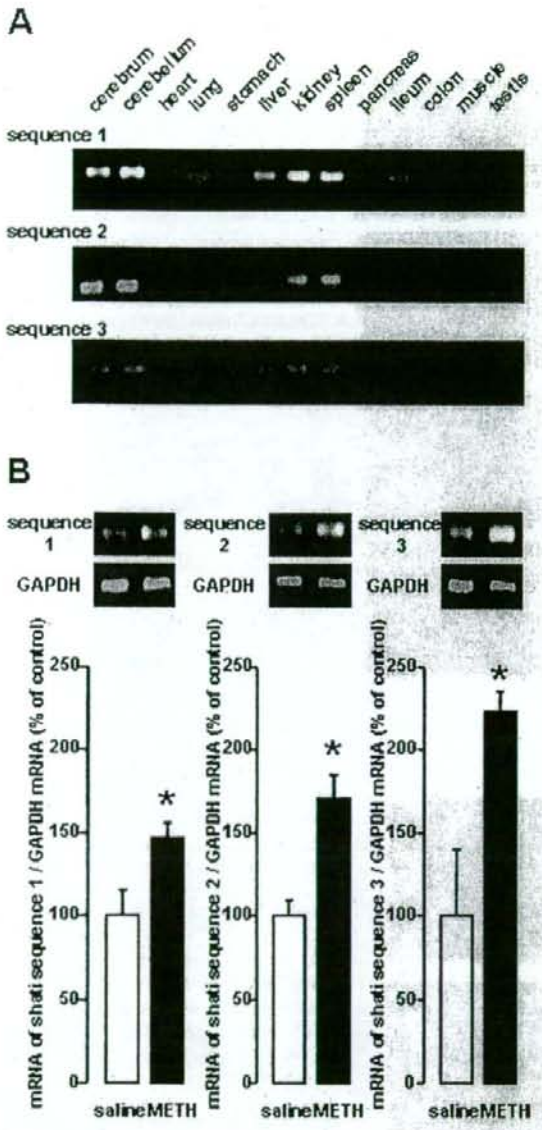

Figure 2. Expression of shati mRNA in the various organs of mice. ***A***, RT-PCR analysis of shati in the various organs in mice. Mice were decapitated without any treatment, and the brains were quickly removed. The sets of primers used for PCR are listed in Table 1. ***B***, Increase in the production of the three sets of target sequences of shati induced by repeated METH treatment in the NAc of mice. Mice were administered METH (2 mg/kg, s.c.) for 6 d and decapitated 2 h after the last METH treatment. Values are means ± SE ($n = 5$). *$p < 0.05$ versus saline-treated mice. The sets of primers used for PCR are listed in Table 1. To standardize the PCR products, we used primers for glyceraldehyde-3-phosphate dehydrogenase (GAPDH) as the internal control.

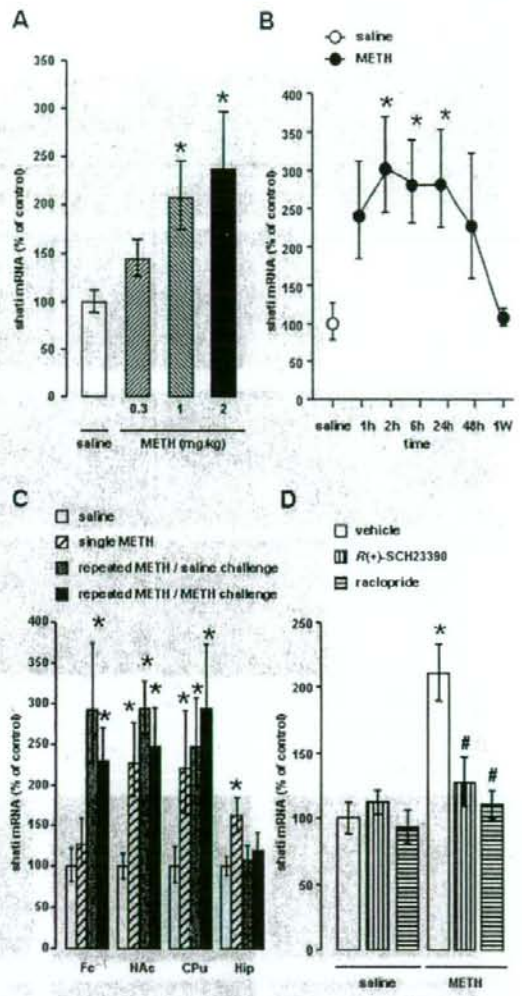

Figure 3. METH induced expression of shati mRNA in the brain. ***A***, Dose-dependent effect of repeated METH treatment on shati mRNA expression in the NAc. Mice were administered METH (0.3, 1, and 2 mg/kg, s.c.) for 3 d. Mice were decapitated 2 h after the last METH treatment. Values are means ± SE ($n = 8$). *$p < 0.05$ versus saline-treated mice. ***B***, Time course changes in the expression of shati mRNA after repeated METH treatment in the NAc. Mice were administered METH (2 mg/kg, s.c.) for 6 d and decapitated 1, 2, 6, 24, and 48 h and 1 week after the last METH treatment. Values are means ± SE ($n = 6–7$). *$p < 0.05$ versus saline-treated mice. ***C***, Changes in the expression of shati mRNA in the various brain regions (Fc, NAc, CPu, and Hip) of the mice after single and repeated METH treatment. Mice were administered METH (2 mg/kg, s.c.) for 5 d and challenged with METH (2 mg/kg, s.c.) or saline on day 6. Mice were decapitated 2 h after last treatment of METH (2 mg/kg, s.c.) or saline challenge. Values are means ± SE ($n = 8–10$). *$p < 0.05$ versus saline-treated mice. ***D***, The effects of the DA D_1-like receptor antagonist *R*(+)-SCH23390 or D_2-like receptor antagonist raclopride on METH-induced expression of shati mRNA in the NAc. Mice were treated with *R*(+)-SCH23390 (0.1 mg/kg, s.c.) or raclopride (2 mg/kg, s.c.) 30 min before daily METH (2 mg/kg, s.c. for 6 d) treatment. Mice were decapitated 2 h after the last METH treatment. Values are means ± SE ($n = 6–8$). *$p < 0.05$ versus vehicle/saline-treated mice. #$p < 0.05$ versus vehicle/METH-treated mice.

0.01 for NAc; single administration, $F_{(1,31)} = 4.917$, $p < 0.05$ for NAc; repeated drug administration × single administration, $F_{(1,31)} = 10.545$, $p < 0.01$ for NAc; repeated drug administration $F_{(1,32)} = 8.023$, $p < 0.01$ for CPu; single administration, $F_{(1,32)} = 4.833$, $p < 0.05$ for CPu; repeated drug administration × single administration, $F_{(1,32)} = 1.669$, $p = 0.206$ for CPu; repeated drug administration, $F_{(1,32)} = 0.628$, $p = 0.434$ for Hip; single administration, $F_{(1,32)} = 6.464$, $p < 0.05$ for Hip; repeated drug administration × single administration, $F_{(1,32)} = 2.496$, $p = 0.124$ for Hip; two-way ANOVA) (Fig. 3*C*). The increase caused by METH in the NAc was inhibited by pretreatment with either the DA